Neural Computing and Applications (2022) 34:16577–16603
https://doi.org/10.1007/s00521-022-07257-7

ORIGINAL ARTICLE

Surrogate modeling for spacecraft thermophysical models using deep learning

Yan Xiong[1,2,3] · Liang Guo[1] · Yang Zhang[1,2] · Mingxing Xu[3,4] · Defu Tian[1,2] · Ming Li[5]

Received: 25 November 2021 / Accepted: 29 March 2022 / Published online: 21 May 2022

Abstract

Thermal modeling is a critical technology in spacecraft thermal control systems, where the complex spatially and temporally variable parameters used as inputs to the spacecraft usually result in long operation times, which hinders sensitivity analysis and control strategies. The uniqueness of both the space environment and the working conditions of each spacecraft, make thermal models differ in different space environments; thus, traditional thermal modeling methods that rely heavily on physical knowledge need to build more than one corresponding thermal model, and they also cannot generalize well. Therefore, an intelligent surrogate modeling strategy for spacecraft thermophysical models that uses deep learning, called SMS-DL, is proposed. An intelligent batch processing system for thermal analysis based on NX TMG Thermal Analysis was designed to automate the input of the thermal design parameters and the output of the thermal analysis results through macro-recording and playback using a state-of-the-art biconjugate gradient solver to provide superior speed, reliability, and accuracy, thus achieving a trade-off between high accuracy and low computational cost. One deep neural network based on Bayesian optimization was pre-trained using the thermal analysis data of the spacecraft in the source domain calculated using a batch processing system, which had a computational speed that was 1000+ times faster than that of the traditional thermophysical model and high computational accuracy of 99%+. Then, it was applied to the target domain with a limited amount of thermal analysis data using model fine-tuning. The theoretical and experimental results from the thermal analysis modeling of the near-ultraviolet radiation detector on the China Space Station Telescope developed in China demonstrated that deep transfer learning effectively adapted the pre-trained model from one working condition to another, improved the prediction accuracy by at least 86.4% over the direct prediction accuracy using the pre-trained model, and had better predictive performance than learning from scratch with only a limited amount of data.

Keywords Surrogate model · Spacecraft thermal design · Thermal analysis · Transfer learning · Deep learning

✉ Liang Guo
guoliang@ciomp.ac.cn

[1] Space Robot Engineering Center, Changchun Institute of Optics, Fine Mechanics and Physics, Chinese Academy of Sciences, Yingkou Road, Changchun 130033, China

[2] Center of Materials Science and Optoelectronics Engineering, University of Chinese Academy of Sciences, Beijing 100049, China

[3] Automatic Control Laboratory, École Polytechnique Fédérale de Lausanne, Lausanne 1025, Switzerland

[4] Department of Electronic Engineering, Shanghai Jiao Tong University, Shanghai 200240, China

[5] Beijing Tiandi Shizhiyuan Trading Company, Beijing 100053, China

1 Introduction

Thermal analysis and simulation are usually performed throughout the entire process of spacecraft development, as well as during the launch and in-orbit operation of the spacecraft [1], and are integral to the development of a spacecraft thermal control subsystem [2]. Spacecraft thermal analysis and simulation mainly use the thermal network method [3], and many practical software programs [4–7] have been developed to play an important role in spacecraft thermal analysis and simulation.

Because of the complexity of the internal structure and layout of spacecraft, acquiring an excessive number of network nodes results in long runtimes [8–10]. Furthermore, long runtimes inhibit the use of models in

applications that involve multiple model runs, such as uncertainty analysis [11, 12], sensitivity analysis [13], and optical-mechanical-thermal integrated modeling [14, 15]. Furthermore, spacecraft typically encounter many different working conditions during in-orbit operation, which leads to thermophysical models differing in different space environments. Thus, traditional thermal modeling methods that rely on physical knowledge need to build more than one corresponding thermal model and cannot generalize well [16]. Therefore, it is of great practical importance to develop cost-effective surrogate modeling methods [17], which have the potential to accelerate complex models without any compromise in accuracy or detail.

Many methods for developing surrogate models exist, such as radial basis functions [18], metamodels [19], simplified models [20], model simulators [21], kriging [22], proxy models [23], and response surface methods [24]. However, these classical methods for modeling surrogate models are mainly suitable for approximation problems with low nonlinearity, whereas it is difficult for them to solve strongly nonlinear and high-dimensional problems. Recently, Mohammadi-Amin et al. [25] proposed a Kriging interpolation and co-Kriging data fusion techniques for surrogate modeling of spacecraft dynamics models, which is one of the most favored surrogate modeling methods in aerospace applications, with applicability to highly nonlinear problems and with more accurate approximations over a wide range of sample size. However, it is like other classical surrogate modeling methods in that it can only accurately fit the original model for a single working condition. If the orbit, internal and external environment of the spacecraft changes significantly, the corresponding dynamical/thermophysical model will change, and the surrogate model built by this method may not fit well with the changed dynamical/thermophysical model. In addition, when the number of parameters associated with the thermophysical model exceeds 50, the effect of the method will become poor, and the time for model evaluation will become too long due to too many parameters, which will defeat the purpose of the surrogate model to improve the computational efficiency.

The deep neural network (DNN) [26, 27] is a promising approach in surrogate modeling because of its ability to handle strong nonlinearities and high dimensionality, which can overcome the curse of dimensionality in certain problems with many great results [28–30]. However, the success of off-the-shelf DNN architectures [31] relies heavily on a large amount of training data and the interpolated nature of the problem, and they fail to work when data become sparse. Unfortunately, tagging data for space thermophysical models are often sparse and can be noisy because they are obtained either from thermal analysis simulations or experimental observations, both of which are expensive [32]. Therefore, in such a "small data" regime, the real power and advantages of DNN cannot be fully exploited by naively using popular off-the-shelf DNN methods from the computer science community to map data and build surrogate models.

Under a specific working condition, a surrogate model based on a DNN can be constructed to approximate the thermophysical model by obtaining a large amount of tagging data through thermal analysis calculation, and after model optimization, good prediction accuracy can usually be obtained [33]. However, when the model switches to a different working condition, such as spacecraft orbit change, the thermal control metrics for some key components of its thermal control system will change, and the infrared radiation emissivity and absorption rates of the system surface materials will also change. In addition, many parameters and boundary conditions related to the thermal analysis modeling will change [34–36], and this will cause the previous DNN-based surrogate model fails to adapt to the thermophysical model for the new working conditions. Obtaining a surrogate model with the same prediction accuracy as the previous condition requires a large amount of tagging data to be generated from scratch for the new condition, which is extremely time-consuming and unfeasible for spacecraft with an excessive number of conditions. Thus, transferability is critical in spacecraft thermophysical surrogate modeling and has not been fully explored yet. Transfer learning has recently received considerable attention and has been successfully applied in various fields, such as indoor localization [37], image processing [38], natural language processing [39], and biological applications [40]. If a model trained in one domain (any variable of interest with a large amount of data) can be adapted to another domain (any variable of interest with limited data), then training the model from scratch can be avoided, and some valuable prior knowledge can be transferred accordingly to improve model learning performance.

To resolve these issues and obtain a thermophysical surrogate model that can be adapted to multiple working conditions, an intelligent surrogate modeling strategy for spacecraft thermophysical models using deep learning called SMS-DL is proposed. To the best knowledge of the authors, this is the first time that transfer learning-based surrogate models that can be adapted to multiple working conditions have been applied to a surrogate thermophysical model for spacecraft. Additionally, SMS-DL differs from traditional surrogate modeling methods because it acquires a large amount of tagging training data for model fitting using time-consuming thermal analysis simulations and can only fit thermophysical models for specific working conditions. It involves the intelligent batch processing system for thermal analysis proposed by Xiong [41] called

IBPS that was based on NX TMG Thermal Analysis [42] and developed by integrating MATLAB and Python. The IBPS can achieve automatic input of thermal design parameters and automatic output of thermal analysis results through macro-recording and playback; and obtain high accuracy thermal analysis results by using the state-of-the-art dual conjugate gradient solver [43]. Thus, it can maximize the accuracy of thermal analysis while minimizing the calculation cost. The system is at least five times faster than traditional manual Monte Carlo estimation [44]. The surrogate modeling method to predict the temperature field designed by Chen [45] and Sun [46] et al. is one of the most important advanced modeling strategies based on DNN used to approximate nonlinear systems, and can speed up model convergence and avoid the excessive demand on the training set. It is used to approximate the thermophysical model as a pre-trained model [47] in the source domain and obtain high-accuracy prediction performance using Bayesian optimization [48]. Then, the parameters from the pre-trained model are adopted to initialize the parameters of the model defined for the target domain and a limited amount of data from the target domain is used to fine-tune the model parameters [49] using a domain adaptation method [50]. The theoretical analysis and experimental results demonstrated that deep transfer learning effectively adapted the pre-trained model from one case to another and improved the prediction accuracy by 67.5% compared with using the pre-trained model directly, while having better prediction performance than learning from scratch using only a limited amount of data, thereby verifying its superiority.

The remainder of the paper is organized as follows: In Sect. 2, the background and motivation of the study are presented. In Sect. 3, details of the SMS-DL design methodology are presented. In Sect. 4, the application of SMS-DL to surrogate modeling for a near-ultraviolet (NUV) radiation detector is presented and the performances of SMS-DL based on transfer learning and the classical DNN-based surrogate modeling method without transfer learning are compared for the interconversion of hot and cold cases. Finally, the results and conclusions of the study are presented in Sects. 5 and 6, respectively.

2 Background and motivation

2.1 Surrogate model

Because space thermal analysis simulations and experiments in the spacecraft thermal design process are very time-consuming and expensive, how to efficiently exchange or fuse data in the spacecraft thermal design process is one of the most popular topics for further research [51]. Surrogate modeling has been widely used as an easy and cost-effective tool to motivate the optimization process of complex system design in general.

Surrogate models usually consist of two components: the design of experiments (DoE) and construction of the surrogate model. Many DoE methods exist, such as uniform design [52], central composite design [53], and Latin hypercube sampling (LHS) [54, 55]. These traditional methods can ensure the uniformity of parameter distribution, but they cannot be updated dynamically as the sampling space size increases, thus making the DoE process inefficient [56]. Progressive LHS (PLHS) proposed by Razi [57] inherits the advantages of traditional DoE methods perfectly and updates the parameter space dynamically as the sampling space size increases, thereby guaranteeing that the sampling space can always form a complete Latin hypercube. Therefore, PLHS is used in this study.

Many methods exist for surrogate modeling, and as described in Sect. 1, and the DNN-based surrogate modelling method is adopted in this study, and a Bayesian optimization algorithm is used to optimize the weights and biases in its network, where the mean square error (MSE) is used as an evaluation metric.

$$\mathrm{MSE} = \sqrt{\frac{1}{m}\sum_{1}^{m}[\hat{y}(x_i) - y(x_i)]^2}, \tag{1}$$

where m denotes the size of the parameter space, x_i denotes the i_{th} set of input parameters, and $y(x_i)$ and $\hat{y}(x_i)$ denote the actual and predicted outputs when the input parameters are x_i, respectively.

2.2 Transfer learning

Transfer learning is an important tool [58] for solving the fundamental problem of insufficient training data in machine learning. It can smartly apply the previous knowledge learned to solve new problems with faster or

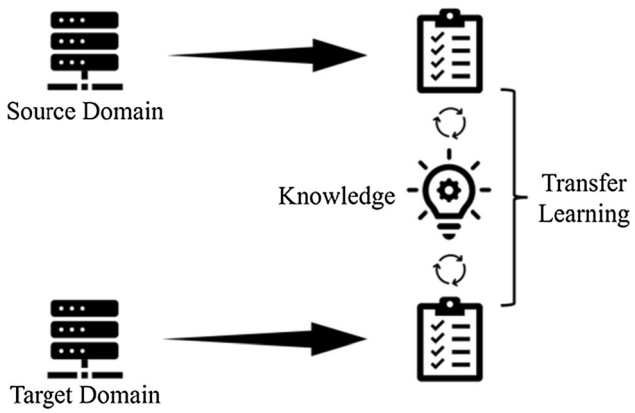

Fig. 1 Learning process of transfer learning

better solutions than traditional approaches that require learning from scratch. This provides a promising approach to many modeling problems that are difficult to improve using optimization because of insufficient training data [59]. Some of the notation used in this paper require clear definitions. First, "domain," "task," "transfer learning," and "deep transfer learning" are defined separately [60].

Definition 1 (*Domain*). A domain is denoted by $D = X, P(X)$, which contains two components: a feature space χ and marginal probability distribution $P(X)$, where $X = \{x_1, x_2, \ldots, x_n\} \in \chi$. In this study, the feature space χ denotes the thermal design parameters of the spacecraft and the marginal probability distribution $P(X)$ denotes the marginal probability distribution of the corresponding output of the feature space. The source domain D_s denotes the working conditions before transfer learning for the surrogate model of the spacecraft thermophysical model and the target domain D_t denotes the new working conditions that need to be optimized using transfer learning for the surrogate model of the spacecraft thermophysical model after it switches working conditions.

Definition 2 (*Task*). A task is denoted by $T = \{y, f(x)\}$, which contains two components: a label space y and target prediction function $f(x)$. In this study, x denotes the thermal design parameters of the spacecraft, the label space y denotes the output data of the thermal analysis obtained from the traditional thermal analysis simulation corresponding to x as the input parameter, and $f(\cdot)$ denotes the prediction function between x and y, that is, the surrogate model. Both learning tasks T_s for the source domain D_s and T_t for the target domain D_t are to obtain the surrogate model of the spacecraft thermophysical model under the corresponding working conditions.

Definition 3 (*Transferlearning*). Given a source domain D_s and its corresponding learning task Ts, together with a target domain D_t and its corresponding learning task T_t, transfer learning aims to improve the learning performance of the target prediction function $f(\cdot)$ in D_t by discovering and transferring knowledge from D_s and T_s, where $D_s \neq D_t$ or $T_S \neq T_t$, typically with the space size of the source domain D_s much larger than that of the target domain D_t.

Definition 4 (*Deeptransferlearning*). Given a source domain D_s and its corresponding learning task T_s, together with a target domain D_t and its corresponding learning task T_t, deep transfer learning is the process of transforming a part of the DNN trained in D_s with its network structure and connection parameters into a part of the DNN used in D_t, reusing it, and thus improving the learning performance of the target prediction function $f(\cdot)$ in D_t by discovering and transferring the knowledge from D_s and T_s through the DNN.

The learning process of transfer learning is shown in Fig. 1.

3 Surrogate modeling for spacecraft thermophysical models using deep learning

In this section, an intelligent surrogate modeling method is presented for spacecraft thermophysical models using deep learning and transfer learning. The process of how to obtain the training dataset required for surrogate modeling using the DoE method is described first. After the training dataset is obtained, a description of how to obtain pre-training models based on the training dataset in the source domain is presented After the working conditions are converted, how to obtain the surrogate model is introduced based on the pre-training model that can be adapted to the new working conditions with limited data using transfer learning. Finally, the practical workflow of SMS-DL is detailed.

3.1 Sample input spaces

As explained in Sect. 2.1, the DoE is a very important and necessary process before surrogate modeling can be performed. Although many DoE methods exist at present, and they have many advantages, the disadvantages are also obvious: they must generate the entire sampling space at once; require the sample size to be specified before sampling; and when it is necessary to continue to expand the sampling space, the expanded sampling space and previous sampling space cannot form a complete Latin hypercube; hence, the original sampling space must be dropped and recalculated, and this greatly increases the calculation cost, which is totally unacceptable for an extremely expensive and complex spacecraft thermophysical model. Thus, as explained in the previous section, PLHS is adopted as the DoE method in this study. It allows the user to observe the effects of sample-based analysis and stop sampling

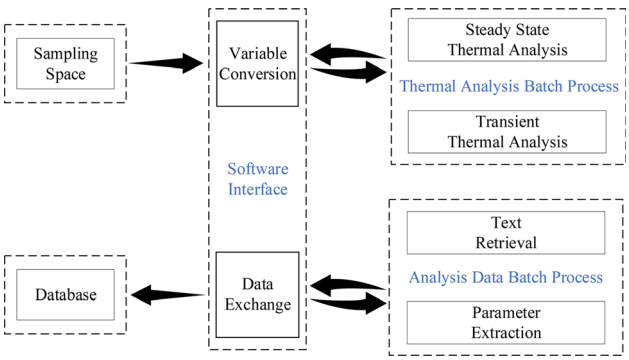

Fig. 2 Workflow of the IBPS [52]

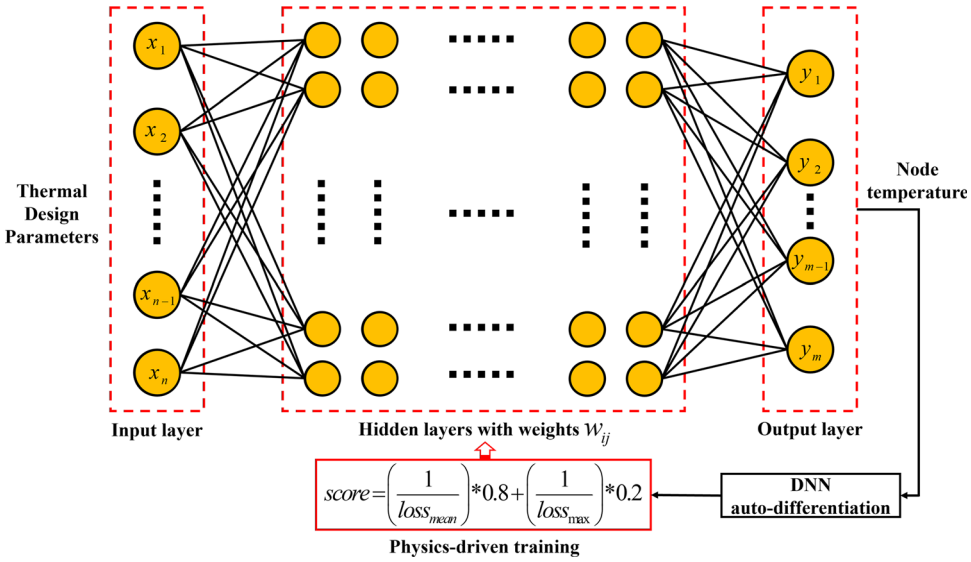

Fig. 3 Schematic diagram of the DNN-based surrogate model

according to actual need, which greatly improves the efficiency of sampling and model evaluation. The mathematical scheme of PLHS is as follows:

$$y_{q,j} = \begin{cases} 1 & \text{If there exist any } i \text{ for which} \\ & x_{i,j} \text{ lies in the interval } q \\ 0 & \text{Otherwise} \end{cases} \tag{2}$$

$S(n, p)$ denotes a sampling matrix with $n \times p$ variables $x_{i,j} \in [0, 1]$, where $i = 1, \ldots, n$, $j = 1, \ldots, p$. Then, a new auxiliary binary variable $y_{q,j}$ is defined:

$$\frac{\sum_{j=1}^{p} \sum_{q=1}^{n} y_{q,j}}{n \cdot p} = 1, \tag{3}$$

Then, $S(n, p)$ satisfies the features of the Latin hypercube when the following equation is satisfied:

$$\sum_{t=1}^{T} \frac{\sum_{j=1}^{p} \sum_{q=1}^{n_t} y_{q,j}^{t}}{n_t \cdot p} = T, \tag{4}$$

Equation (3) can be regarded as the summation of Eq. (2); hence, the PLHS generated by the above mathematical formulation can be regarded as an optimization problem as follows:

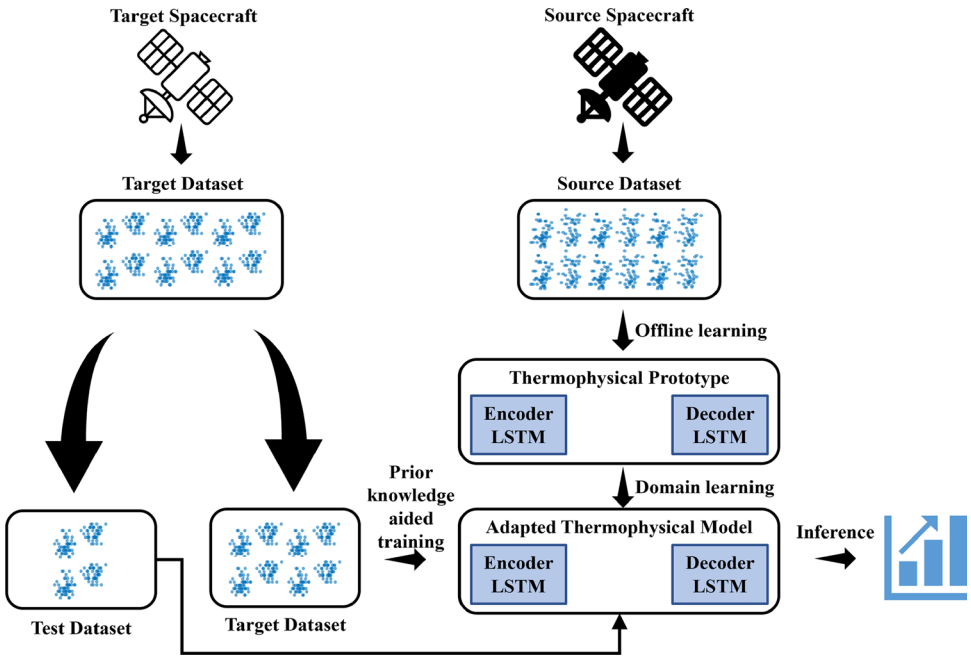

Fig. 4 Schematic diagram of the fine-tuning model based on transfer learning

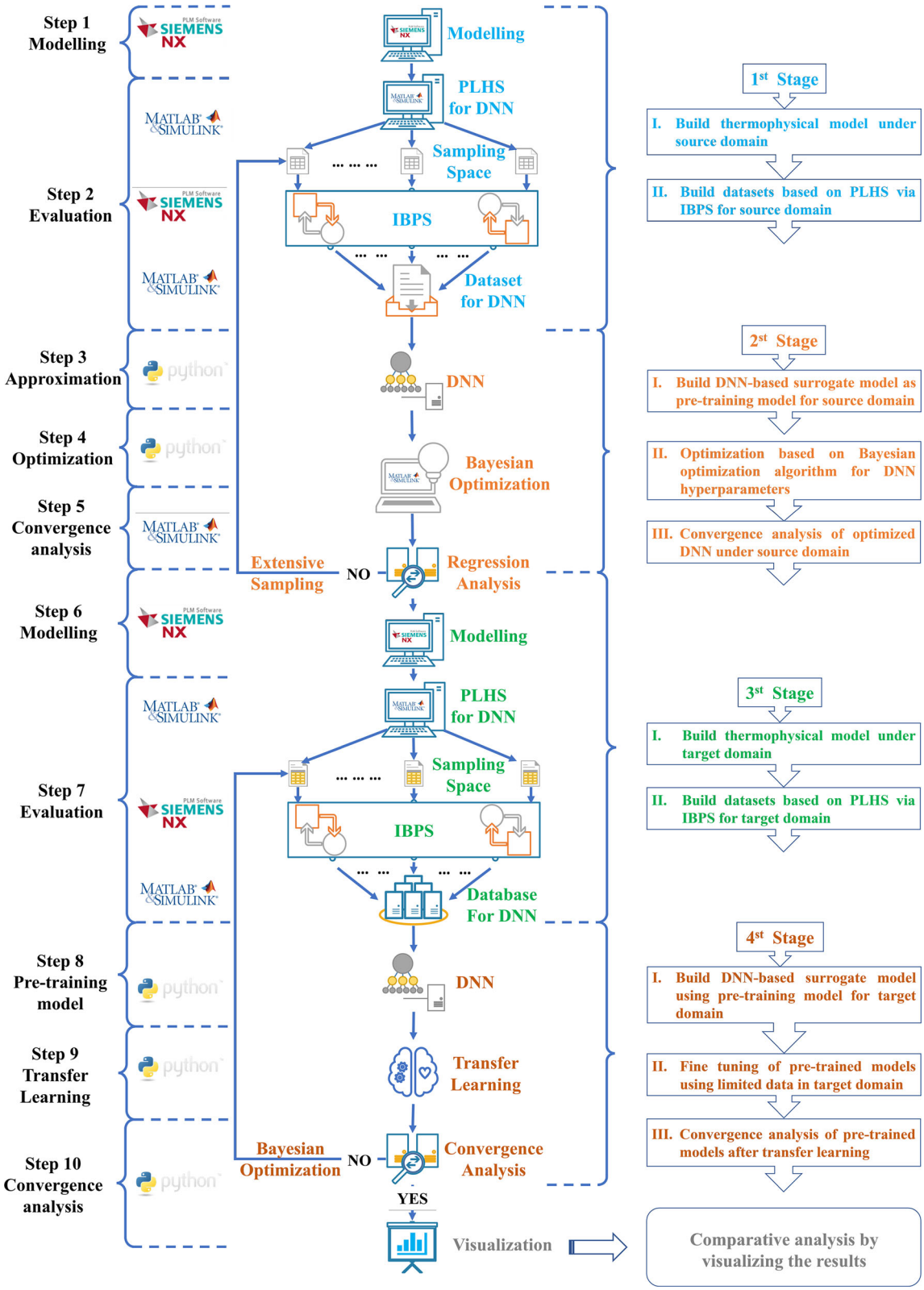

Fig. 5 Practical workflow of SMS-DL

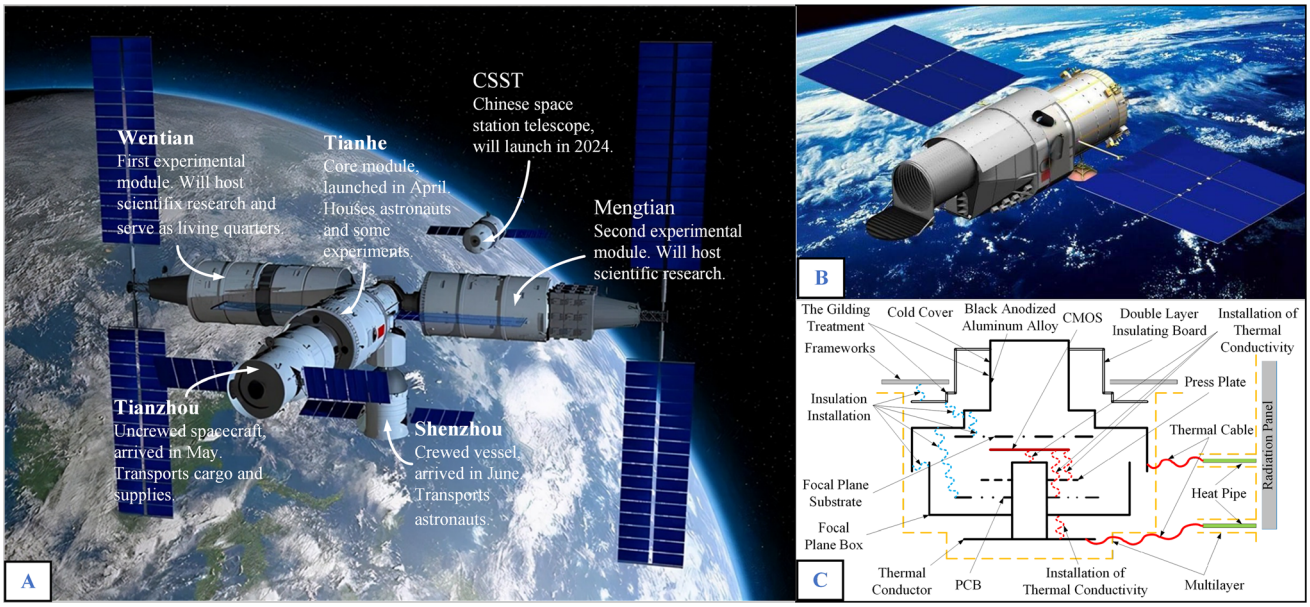

Fig. 6 Overall structure of the CSS and CSST. **A** Overall structure of the CSS. **B** Overall structure of the CSST. **C** Structural diagram of the SCI700 detector [62–64]

Table 1 Comparison of contemporary survey space telescope projects

Project Name	CSST	Euclid	RST
Orbit	Low earth orbit	Lagrangian point L2	Lagrangian point L2
Aperture (m)	2	1.2	2.4
Mass (kg)	15,500	2160	6330
Launch	2024	2022	2025
Field of view (square degree)	1.1	0.55/0.56	0.28
R_{EE80} ($''$)	0.15	0.23/0.63	0.24
Number of pixels (100 million)	31	6.1/0.7	3
Survey area (m^2)	17,500	15,000	2000
Wavelength (nm)	255–1000	550–900/920–2000	927–2000
Number of imaging bands	7	1/3	4
Number of spectral bands	3	None/1	1

Table 2 Parameters and settings of the orbital environment

Parameter	Hot case	Cold case
Orbit	Low earth orbit	
Minimum altitude	400 km	
Satellite position	Local time at Ascending Node 18:00:00	
Orbit period	5544.9 s	
Orbit inclination	98.38°	
Albedo	0.306	
CMOS power	0.65 W	
System heating power	$\leq$ 120W	
Temperature Index for frameworks	19–25°C	
Stefan–Boltzmann constant	5.67×10^{-8} W/($m^2 \cdot K^4$)	
Solar constant	1411 W/m^2	1323 W/m^2
Earth IR	237 W/m^2	220 W/m^2

Table 3 Average external heat flux of the CSST in hot and cold cases. (Unit: W/m^2)

Surface		$+X$	$+Y$	$+Z$	$-X$	$-Y$	$-Z$
June	Q_{sun}	285.1	0	35.1	287.1	0	402.8
	$Q_{\text{E-air}}$	58.9	58.9	181.0	58.9	58.9	0
	Q_{ref}	33.7	33.5	103.2	33.6	33.5	0
December	Q_{sun}	304.1	0	37.5	305.7	0	430.8
	$Q_{\text{E-air}}$	72.7	72.7	223.0	72.7	72.7	0
	Q_{ref}	43.5	43.3	133.4	43.5	43.3	0

$$\text{Maximize}\left(\sum_{t=1}^{T}\frac{\sum_{j=1}^{p}\sum_{q=1}^{n_t}y_{q,j}^{t}}{n_t\cdot p}\right), \tag{5}$$

where $x_{i,j}$ is a decision variable and $y_{q,j}^{t}$ is an auxiliary variable.

3.2 Intelligent batch processing system for thermal analysis

The thermal physics model of a spacecraft has many types of thermal design parameters, and to determine the best solution for the thermal design of a spacecraft, the traditional method of spacecraft thermal control requires the thermal engineer to manually import these parameters into thermal analysis software and perform a great deal of repetitive work, from which the thermal engineer needs to obtain and analyze the effect of different modeling parameters on the thermal analysis results. Clearly, this requires a great deal of repetitive work, is extremely time-consuming, and would be very error-prone if the output data were imported and collected purely manually. Therefore, as explained in Sect. 1, in this study, IBPS developed by Xiong is used. This system can automatically create a sampling input space, and perform batch thermal analysis and automatic extraction of the result data without supervision, which greatly improves the efficiency of thermal analysis and avoids the high cost and possibility of errors caused by manual labor.

IBPS has several powerful functional modules, such as thermal design parameter sampling, parameter loading, and space thermal analysis result extraction, which are developed based on MATLAB [61]; see Fig. 2 for details.

Table 5 Surface processes and their thermophysical properties

Name	Solar absorptivity	Infrared emissivity
Black anodizing	0.80–0.95	0.80–0.95
Gold plating	0.15–0.40	0.02–0.05
S781 white coatings	0.12–0.25	0.80–0.94
F46	0.11–0.45	0.60–0.80

3.3 Pre-training model based on deep learning

After the sampling space under a given working condition (source domain) is obtained using IBPS, the DNN architecture is first required to approximate the spacecraft thermophysical model, that is, the DNN-based surrogate model of the spacecraft thermophysical model, which is optimized using the Bayesian optimization algorithm to improve the fitting accuracy. After offline training, this surrogate model quickly generates corresponding temperature predictions online and in real time given any combination of spacecraft thermal design parameters. Because the following transfer learning is used to build the surrogate model based on this model to adapt to new working conditions (target domain), this model is referred to as the pre-training model, that is, the model that prepares for the next round of transfer learning.

The schematic diagram of the DNN-based surrogate model is shown in Fig. 3.

Table 4 Materials used in the detector and their physical properties

Name	Material	Density kg/m^3	Thermal conductivity W/mK	Specific heat capacity J/kgK
Focal plane box	Aluminum alloy (2A12)	2780	121	921
CMOS	Photosensitive material	1800	20	500
PCB	Composite materials	1800	20	500
Thermal conductor	Aluminum alloy (7A09)	2850	134	921
Thermal cable	Copper	8750	350	400
Cold cover	Aluminum alloy (7A09)	2850	134	921
Insulation pads/rings	Polyimide	1420	0.25	1130

Table 6 Description and range of the thermal design parameters

	Parameter description	Base value	Lower limit	Upper limit
	Inner surface of the cold cover	0.84	0.80	0.95
	Outer surface of the cold cover	0.25	0.15	0.40
Solar	Radiation panel	0.18	0.12	0.25
absorptivity	Inner surface of double layer insulating board	0.84	0.80	0.95
	Outer surface of double layer insulating board	0.25	0.15	0.40
	Inner surface of focal plane box	0.84	0.80	0.95
	F46	0.41	0.11	0.45
	Inner surface of the cold cover	0.84	0.80	0.95
	Outer surface of the cold cover	0.05	0.02	0.05
Infrared	Radiation panel	0.87	0.80	0.94
emissivity	Inner surface of double layer insulating board	0.84	0.80	0.95
	Outer surface of double layer insulating board	0.05	0.02	0.05
	Inner surface of focal plane box	0.84	0.80	0.95
	F46	0.68	0.60	0.80
	Between thermal cable and thermal conductor	1.11	0.13	2.5
	Between thermal cable and cold cover	0.23	0.13	2.5
	Between thermal cable and heat pipe	1.23	0.13	2.5
	Between heat pipe and thermal cable	0.67	0.13	2.5
	Between thermal conductor and CMOS	4.22	1.48	4.44
	Between thermal conductor and focal plane box	1.18	0.71	3.53
	Between cold cover and insulation pads	3.79	2.28	25
	Between cold cover and PCB	201.81	21.4	273.14
	Between cold cover and double layer insulating board	68.42	3.98	81.68
Thermal	Between cold cover and focal plane box	11.74	1.86	38.01
resistance	Between double layer insulating board and framework	68.42	3.98	81.68
	Between double layer insulating board and external insulation ring	5.00	0.63	10
	Between double layer insulating board and internal insulation ring	5.00	0.47	10
	Between external insulation ring and framework	15.00	2.5	25
	Between internal insulation ring and cold cover	5.00	2.10	10.47
	Between focal plane box and CMOS	6.93	4.16	40
	Between focal plane box and insulation pads	3.79	2.28	40
	Between focal plane box and press plate	3.89	2.34	40
	Between CMOS and press plate	12.15	7.29	66.67
	Between CMOS and PCB	4.47	2.68	13.42
	Internal insulation ring	2.35	1	5
Thickness	External insulation ring	2.91	1	5
	Insulation pads	1.24	1	5
Heat transfer coefficient	Between multilayer and wrapped area	0.17	0.05	0.6
	Thermal conductor	154.00	100	250
Thermal	Thermal cable	300.00	150	300
conductivity	Cold cover	154.00	100	250
	Focal plane box	154.00	100	250

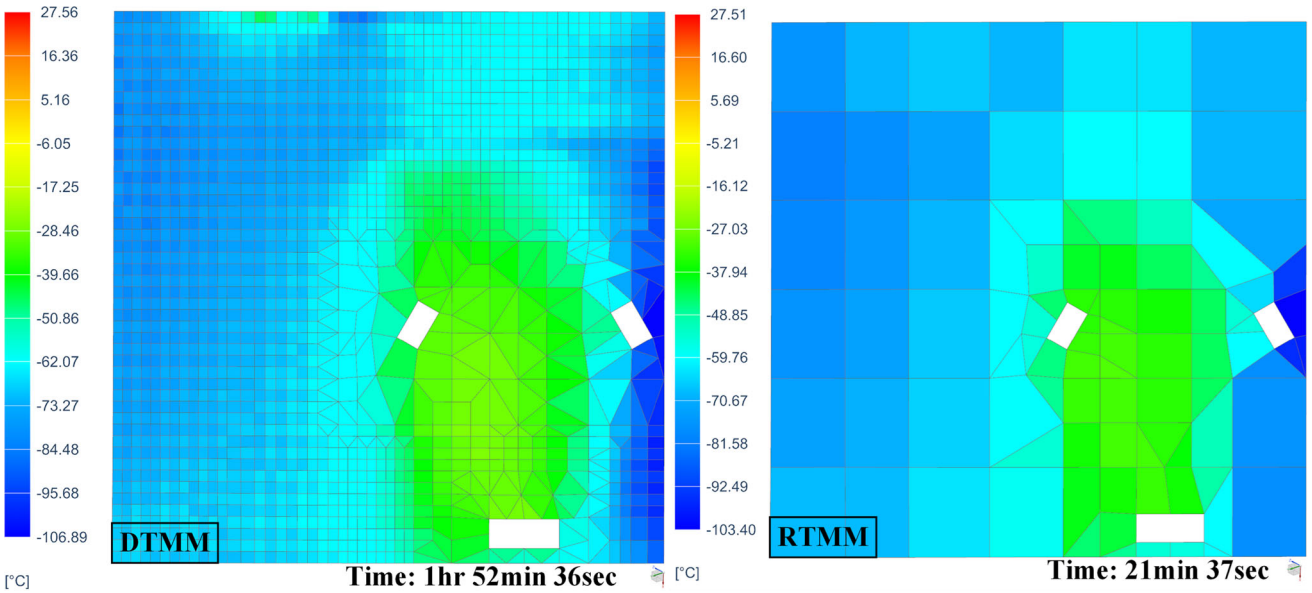

Fig. 7 Thermal analysis cloud map of support plate of the CSST main mirror

3.4 Fine-tuning model based on transfer learning

After the DNN-based surrogate model is pre-trained with a large amount of tagging data from the source domain, the model parameters in the source domain are used to initialize the model parameters in the target domain, thereby maintaining the same structure of the DNN, and all the parameters of the model in the source domain are kept as the initialization parameters of the model in the target domain, except for the output layer weights; that is, after the model is initialized in the target domain based on the pre-trained model, the parameters of its encoder and decoder are not updated, and then the limited tagging data in the target domain are used to fine-tune and optimize the output layer weights of the pre-trained model, thus achieving faster and better adaptation to the target domain through transfer learning than learning from scratch with only a limited amount of data in the target domain while inheriting the advantages of the pre-trained model in the source domain. The schematic diagram of the fine-tuning model based on transfer learning is shown in Fig. 4.

Compared with modeling in the target domain from scratch using DNN, the fine-tuning model based on transfer learning is faster and better adapted to the target domain with limited tagging data, which greatly reduces the cost for surrogate modeling and improves efficiency simultaneously.

3.5 Practical workflow of SMS-DL

The proposed SMS-DL has four stages and 10 steps. Two programming languages and space thermal analysis software are used (Fig. 5).

Stage 1: The thermophysical model of the spacecraft in the source domain is established using the thermal network

Table 7 Comparison analysis of the effect of different sampling space sizes for DNN accuracy

Sampling size	MSE	
	Hot case	Cold case
500	2.1632	1.9842
5000	1.6044	0.9433
10,000	0.7829	0.1675
15,000	0.0709	0.0675
20,000	3.35e–3	5.41e–3
25,000	7.63e–4	6.59e–4
30,000	6.51e–4	5.89e–4
35,000	5.16e–4	6.09e–4
40,000	5.12e–4	6.01e–4
45,000	5.09e–4	5.97e–4
50,000	5.11e–4	6.08e–4
55,000	7.35e–4	8.87e–4
60,000	8.58e–4	9.02e–4
65,000	1.37e–3	1.81e–3
70,000	3.06e–3	4.74e–3

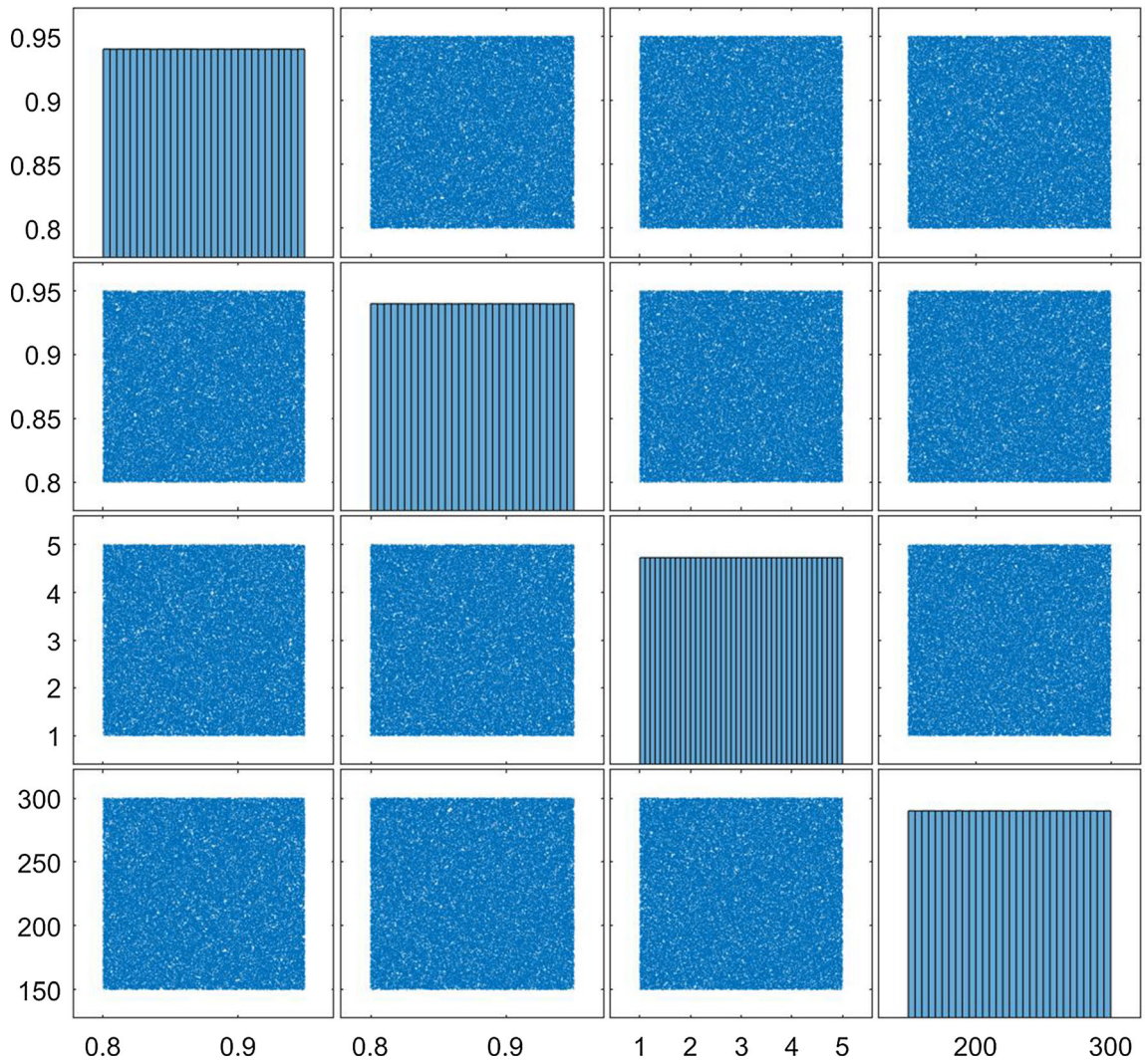

Fig. 8 Distribution of the DoE samples in the source domain

method. Then, sampling is performed within the range of the thermal modeling parameters to create a sample input space based on the PLHS method to use as training data for the source domain, and the thermophysical model of the spacecraft is imported using IBPS for space thermal analysis in batch mode, thereby maintaining the accuracy of the model output without supervision.

Stage 2: A DNN is first used to approximate the spacecraft thermophysical model computed using IBPS as a pre-training model, while the DNN-based surrogate model greatly accelerates post-processing. Then, the hyperparameters of the DNN are optimized using the Bayesian optimization algorithm to improve performance. Finally, convergence analysis is performed to evaluate the fitting performance of the DNN and determine whether the sampling space should be extended further or the hyperparameters should be optimized further.

Stage 3: The thermophysical model of the spacecraft in the target domain is first built using the thermal network method. Then, sampling is performed within the thermal modeling parameters to establish a sample input space using the PLHS-based method as training data in the target domain, and the thermophysical model of the spacecraft is imported using IBPS for batch space thermal analysis to maintain the accuracy of the model output in an unsupervised manner.

Stage 4: First, the surrogate model based on DNN for spacecraft's thermophysical model is initialized in the target domain using the structure and hyperparameters of the pre-training model and all the network parameters are fixed, except for the output layer, that is, the regression prediction layer weights. Then, the pre-trained model is trained using the limited training data in the target domain. Finally, convergence analysis is performed to evaluate the fitting performance of the DNN in the target domain after

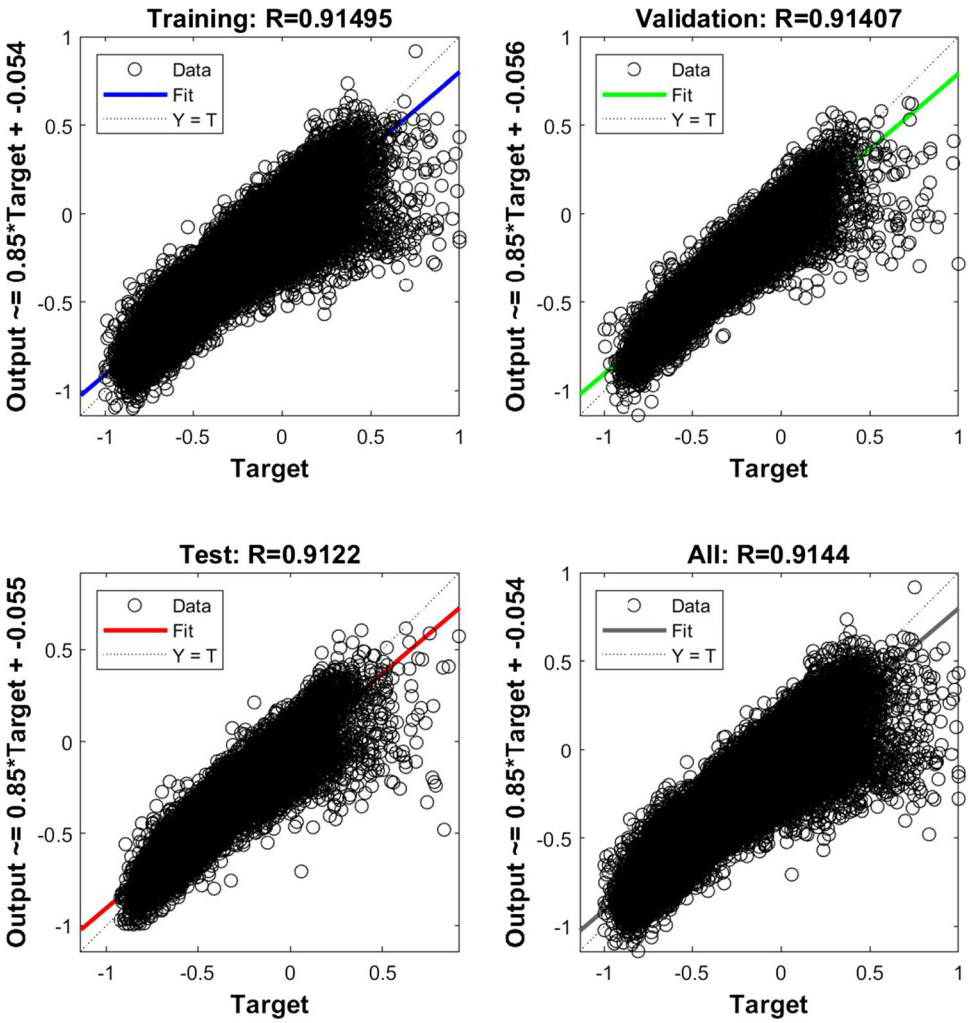

Fig. 9 Regression of the established DNN in the source domain without optimization

transfer learning and to determine whether further hyperparameter optimization is required.

4 Example applications

To validate its performance, SMS-DL was applied to surrogate modeling for the multi-condition thermophysical model of the NUV detector of the China Space Station Telescope (CSST) designed and manufactured by the Chinese Academy of Sciences (CAS) and China Academy of Space Technology (CAST), and the results were analyzed in a multidimensional manner.

In this section, the application of SMS-DL to the CSST is presented in detail. First, the background of the CSST is presented. Then, the thermophysical model of the CSST is described. Furthermore, the proposed SMS-DL is used to adapt the surrogate model of the CSST thermophysical model in hot and cold working conditions under different working conditions using transfer learning. Finally, the performance of SMS-DL is analyzed in multiple dimensions before and after working conditions are switched to verify its excellent performance in the surrogate modeling of thermophysical models under multiple working conditions.

4.1 Background of the CSST

To conduct wide-field multiband imaging and seamless spectroscopic surveys, and in-depth studies of selected objects or regions of space, such as dark forces, dark matter, gravity theory, and the Hubble constant, using multiple observation tools, CAS and CAST have jointly designed a new 2 m aperture space telescope, which shares the same orbit as the Chinese manned space station and will facilitate the maintenance of equipment by docking with the station when necessary. The overall structure of the CSST is shown in Fig. 6A. It is equipped with a survey camera, terahertz receiver, multichannel imager, integral field spectrograph, and cool-planet imaging coronagraph. As shown in Table 1, several survey space telescope projects exist, and clearly, the CSST is not only substantially

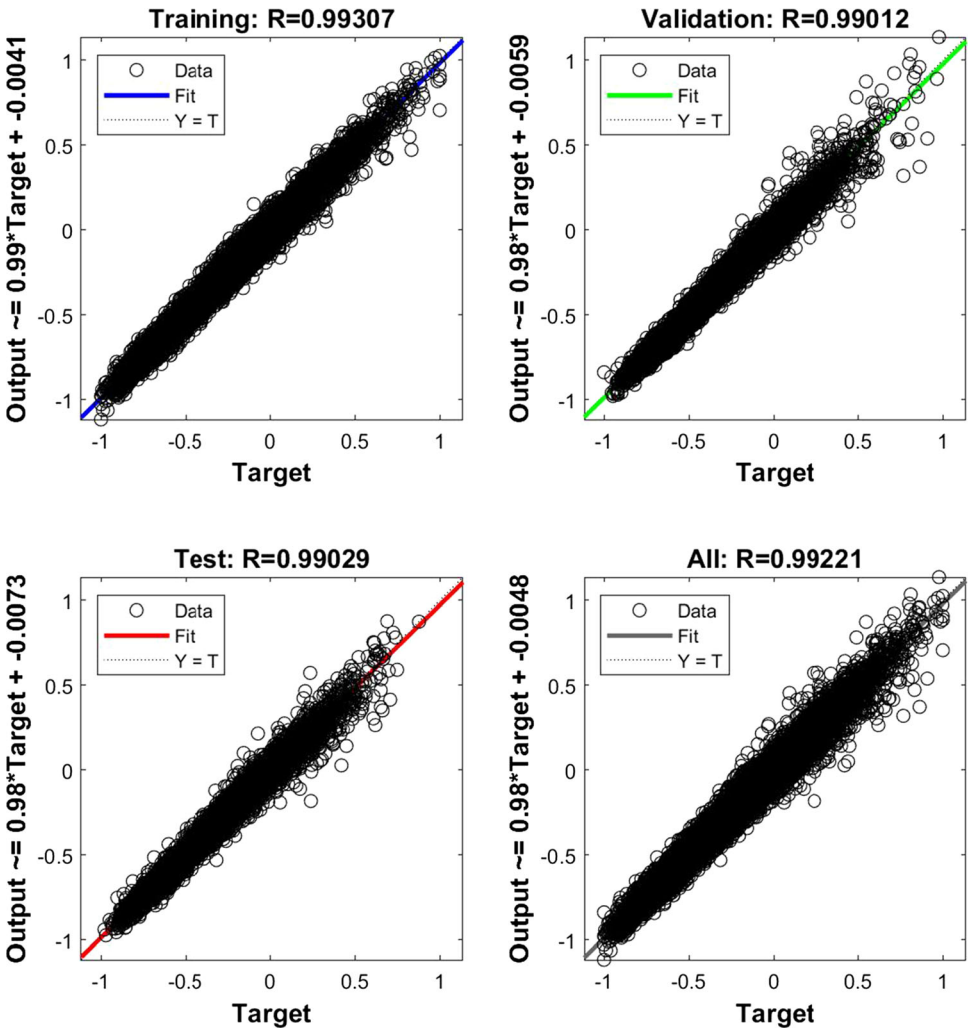

Fig. 10 Regression of the pre-training model in the source domain after optimization

better than previous projects in many aspects, including the metrics of large-scale multicolor imaging and seamless spectral surveys, but also has the best image quality among contemporaneous projects, especially in the NUV band, which is unique, with excellent overall performance and very competitive. SCI700 is a core NUV detector in the CSST and is essential for observing and studying the dynamics of NUV from stars in the 700 nm band.

The parameters and settings of the orbital environment are presented in Table 2, which indicate that the CSST works in a low earth orbit at 400 km altitude, exposed to a complex thermal environment, including the heat flux from direct sunlight (Q_{sun}), infrared radiation from the earth ($Q_{\text{E-air}}$), and sunlight reflected from the earth (Q_{ref}), details shown in Table 3). Based on the effects of these heat fluxes and the internal heat sources of the spacecraft, etc., a heat balance equation for the spacecraft can be obtained as follows:

$$\rho C_{\text{P}} \frac{\partial T}{\partial t} = Q_{\text{sun}} + Q_{\text{ref}} + Q_{E-\text{air}} + Q_{\text{n}} - (Q_{\text{rad}} + Q_{\text{conv}} + Q_{\text{cond}}) \tag{6}$$

where

$$Q_{\text{sun}} = \alpha_{\text{s}} \cdot S_0 \cdot \varphi_1 \tag{7}$$

$$Q_{\text{ref}} = \alpha_{\text{s}} \cdot \varphi_2 \cdot R \cdot S_0 \tag{8}$$

$$Q_{\text{E-air}} = \varepsilon_1 \cdot \frac{1-R}{4} S_0 \cdot \phi_3 \tag{9}$$

where ρ, C_{p} are the density and specific heat capacity of the spacecraft material, respectively; α_{s} is the solar radiation absorption rate at the spacecraft surface; S_0 is the solar constant; φ_1 is the view factor of the spacecraft surface to direct solar radiation; φ_2 is the view factor of the spacecraft surface to the Earth's albedo radiation; R is the ground average reflectance; ε_1 is the infrared emissivity of the material on the external surface of the spacecraft; φ_3 is the view factor of Earth infrared radiation; Q_{n} is the power of the internal heat source of the spacecraft system; Q_{rad} is the

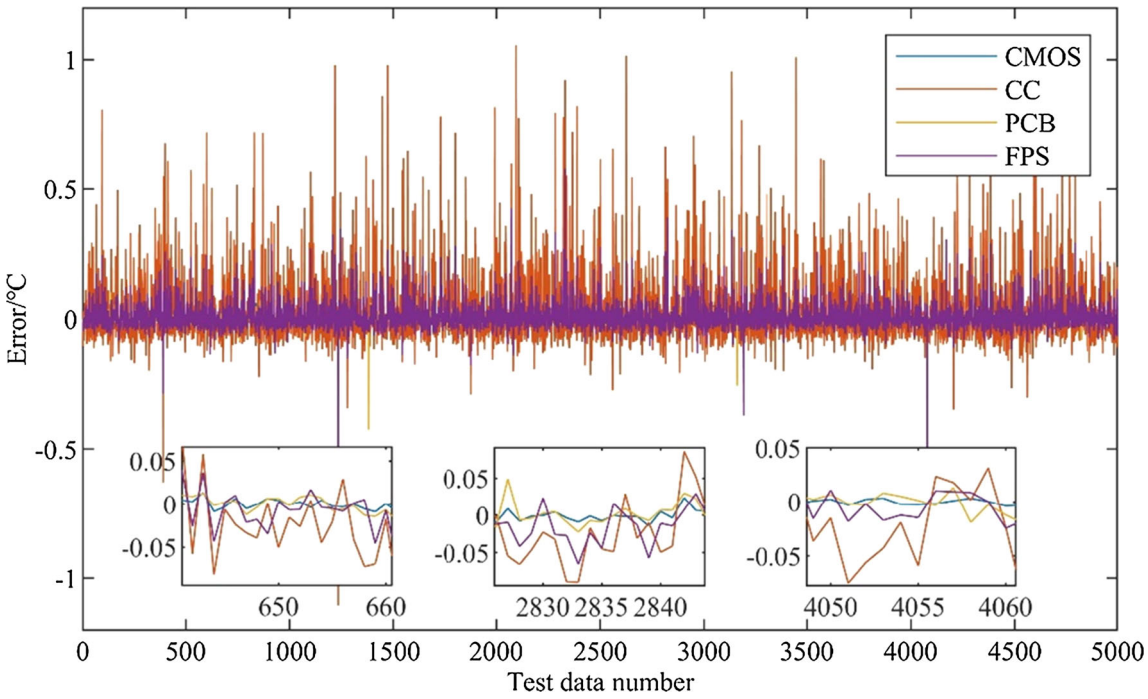

Fig. 11 Evaluation of the optimized pre-training model in the source domain

radiation heat exchange between the spacecraft and the surrounding environment; Q_{conv} is the convective heat exchange between the spacecraft and the surrounding environment; Q_{cond} is the conduction heat exchange between the spacecraft and its surrounding environment.

Additionally, the heat flux between the sunlit and shadowed surfaces varies greatly, which may lead to a non-uniform temperature distribution between the primary mirror and the detector, thus compromising the imaging quality of the CSST. Because of the length limitation, only the SCI700 NUV detector is studied in this paper, and its structure and thermal transfer path are shown in Fig. 6B and C. Simultaneously, the predicted outputs of the SMS-DL-based surrogate model are the node temperatures of four critical components: the CMOS, cold cover (CC), PCB, and focal plane substrate (FPS). Table 4 shows the materials used in the detector and their physical properties, which are influenced by manufacturing and processing (see Table 5). Table 6 shows the description and range of values for the 42 thermal design parameters of the LHS, which are feature parameters shared by both hot and cold cases. Because of the complexity and variability of the space environment, the CSST requires high thermal control accuracy during both storage and runtime; hence, Xiong et al. proposed a novel intelligent thermal control scheme based on deep reinforcement learning [65], and it works very well. In this study, the thermophysical model of the CSST is built based on this scheme using the thermal network method.

4.2 Thermophysical model of the CSST

As mentioned in Sect. 4.1, traditional spacecraft thermal control methods usually use the finite element method to construct a thermophysical model and calculate the temperature field of the spacecraft. The increase in the number of finite element meshes directly affects the accuracy of the thermal analysis and increases the computational time significantly. When the number of finite elements meshes exceeds a certain threshold, it will lead to the bottleneck problem that the computational time increases sharply without increasing the computational accuracy. Therefore, it is necessary to plan the mesh size and number of each component on the spacecraft reasonably to trade-off the computational accuracy and efficiency.

Based on the three-dimensional model of the CSST and the thermal control scheme, the original thermophysical model of the CSST was built using NX TMG Thermal Analysis software, which had 19,370 cells, 20,607 nodes, and 223 thermal couplings, as shown in Fig. 7 for the support plate of the CSST main mirror.

As traditional spacecraft thermal analysis typically uses the Monte Carlo ray tracing method to evaluate thermal radiation [66], which is very expensive and requires many computational resources, the thermal model reduction is

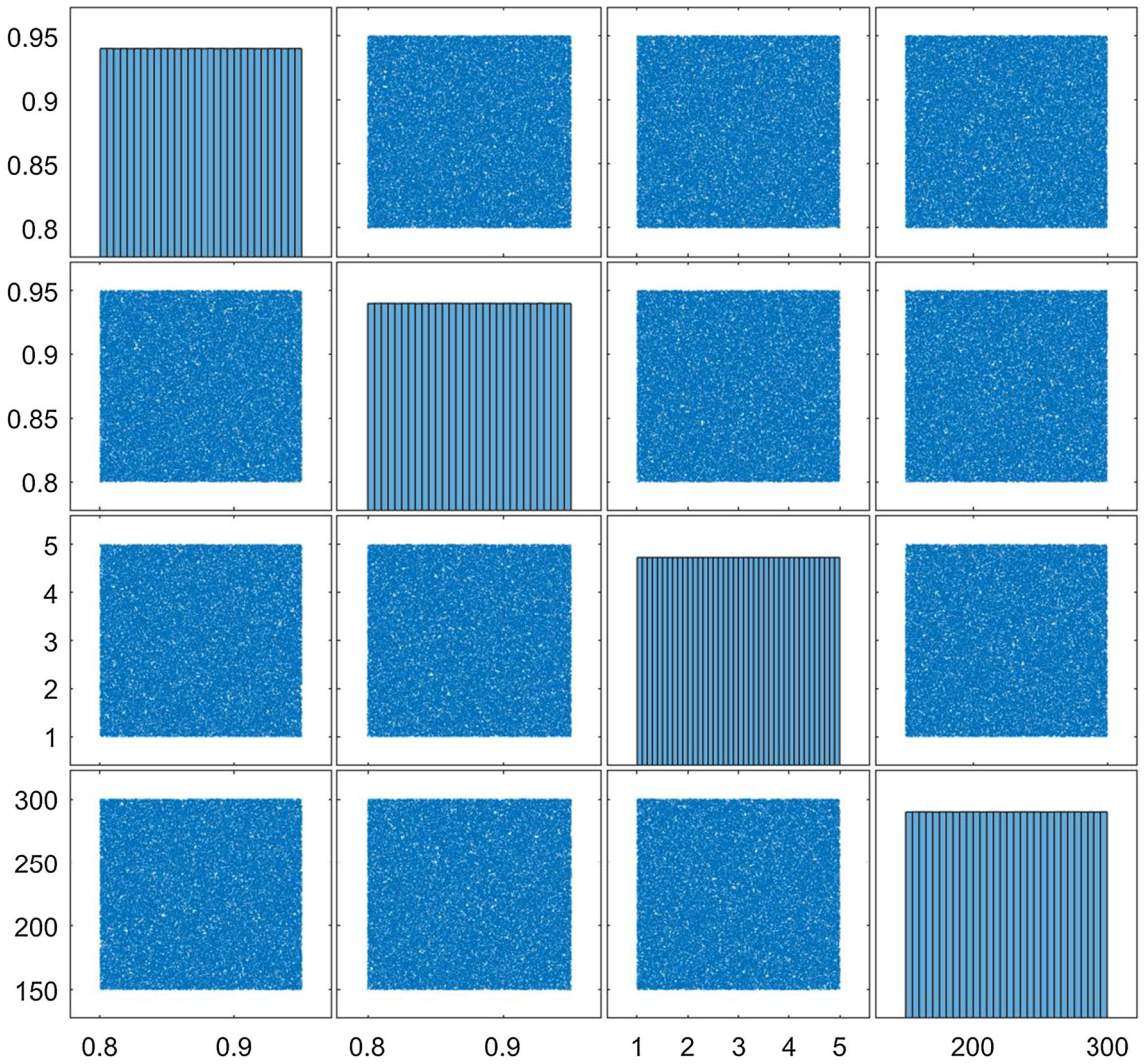

Fig. 12 Distribution of the DoE samples in the target domain

widely used to improve the efficiency of thermal analysis. In this study, the thermal model reduction strategy proposed by Michael [67] was used to obtain a reduced thermal mathematical model (RTMM) by applying reduction correlation using the detailed thermal mathematical model (DTMM) of the CSST. The simulation time of RTMM with 6310 cells and 6885 nodes was reduced by 80.8% compared with that of DTMM, and the temperature difference between RTMM and DTMM for the steady-state thermal analysis results was less than 2K, which was acceptable in the initial thermal design of the CSST; hence, RTMM was used for thermal analysis in the next batch thermal analysis, which is fully acceptable for aerospace engineering requirements.

4.3 Application of SMS-DL

4.3.1 Surrogate model based on the DNN in the source domain

In this study, to improve the verification of the generalizability of SMS-DL, two cases were considered, Case 1 and Case 2, which are explained below.

Case 1: The hot case was considered as the source domain and the cold case as the target domain. Then, a DNN-based surrogate model in the source domain was built as a pretraining model and its hyperparameters were optimized using a Bayesian optimization algorithm, which was developed by Ray.tune [68], and is an excellent toolbox for hyperparameter optimization based on Python.

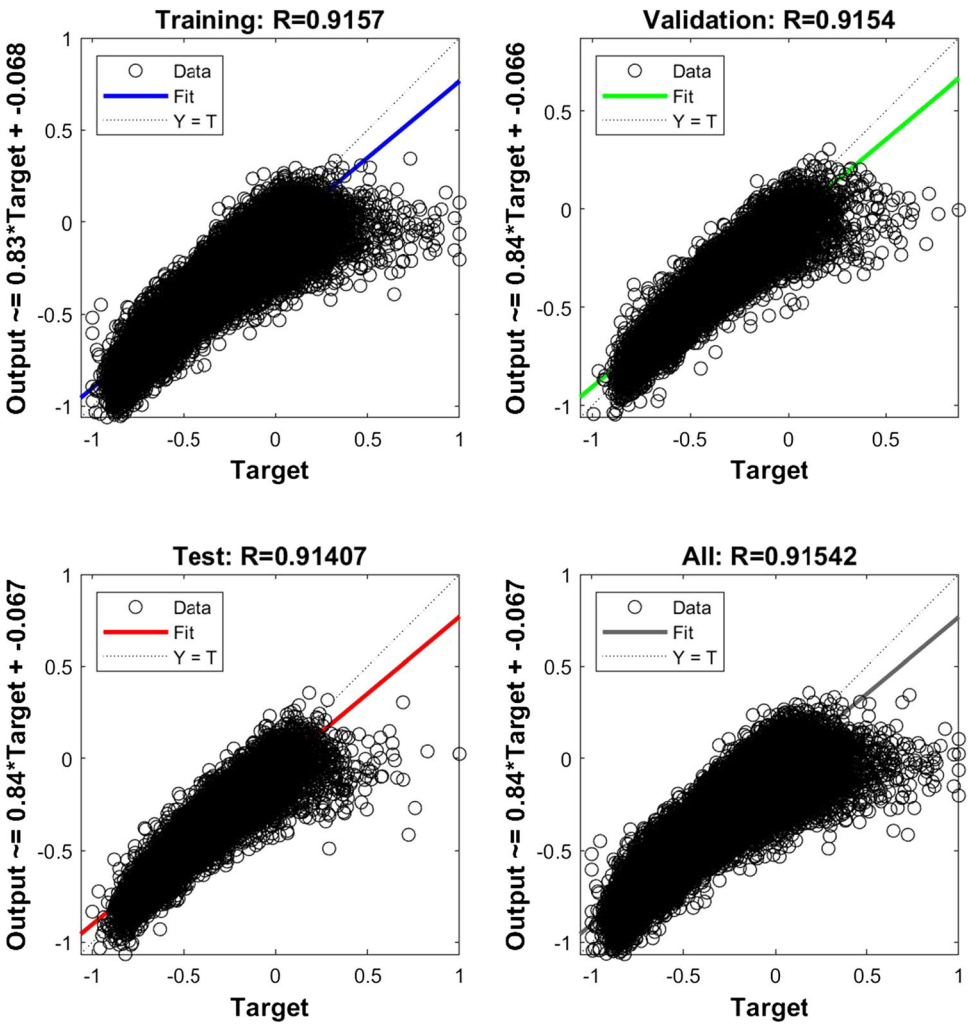

Fig. 13 Regression of the established DNN in the target domain without optimization

Before surrogate modeling, it was necessary to create a sampling space. Generally, the larger the sampling space, the better; however, building a sampling space is very time-consuming and laborious; hence, it was necessary to first make a trade-off in terms of computational efficiency and accuracy to obtain the optimal sampling space. For this purpose, a DNN was established and trained on different sizes of sampling space. Table 7 clearly shows that the MSE of the neural network decreased sharply and the average error decreased as the sampling space size increased from 500 to 20,000, which indicates that the increase in the amount of training data helped to further optimize the model. However, from 20,000 to 45,000, the MSE of the neural network did not change significantly, and although the average error decreased, it was not obvious; hence, the further increase of the training data at this stage no longer played a critical role in improving the accuracy of the model. More critically, from 45,000 to 50,000, the MSE and average error of the neural network tended to increase, which indicates that the increase of the training data led to the overfitting of the model after a certain degree. Therefore, after a comprehensive evaluation, 50,000 groups within the value range of the 42 thermal design parameters were sampled, as shown in Table 6, using PLHS as the sampling input space. The distribution of some parameters is shown in Fig. 8. The probability distribution laws of the parameters not shown in Fig. 8 were consistent with those of the parameters in Fig. 8. Then, thermal analysis batch processing was performed in the source domain using IBPS; thus, the dataset for surrogate modeling in this source domain (42 inputs to 4 outputs) was obtained and stored in text format in an Excel file on the specified path. This process took 56 days.

Next, 80% of the dataset was used as a training set for surrogate modeling, 10% for validating the generality of the network, and the remaining 10% for testing. In this study, the torch.nn.Module in PyTorch [69] was used to build the DNN, which allowed the construction and management of complex neural network structures. Based on the surrogate modeling method proposed by Xiong et al.

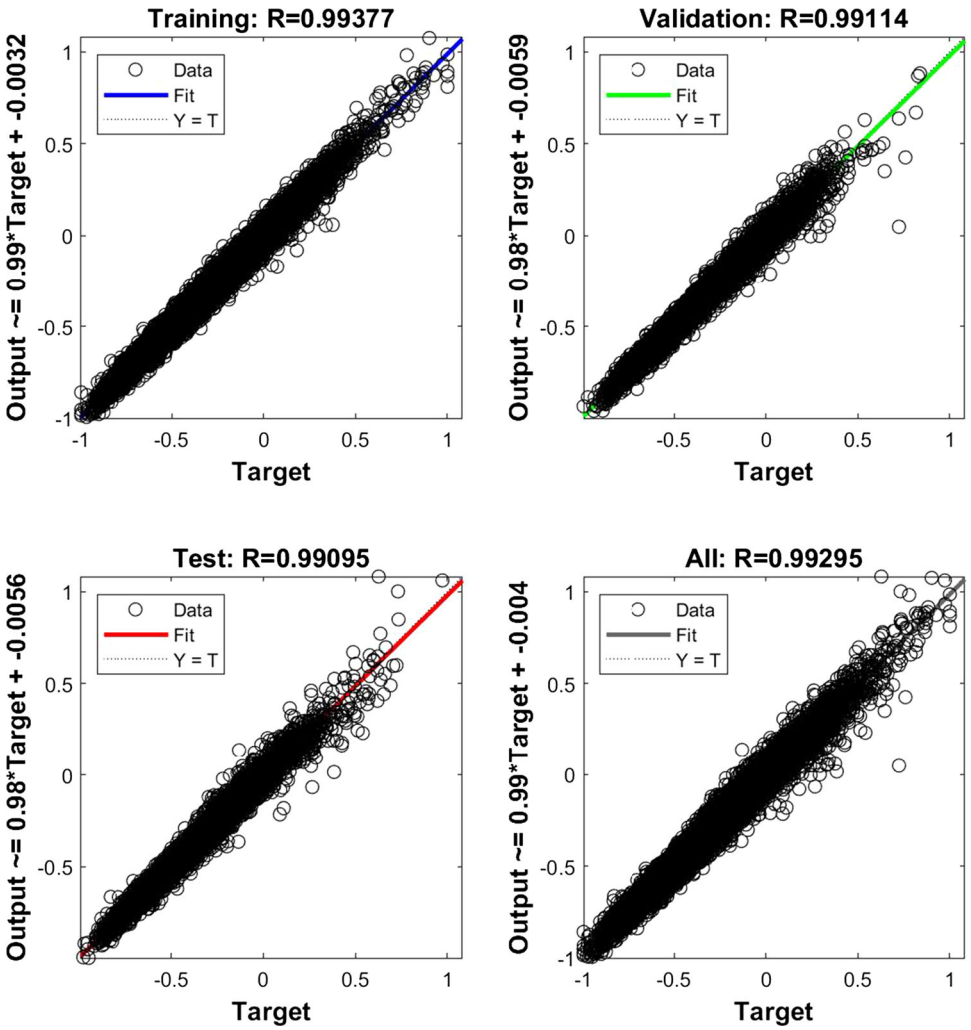

Fig. 14 Regression of the pre-training model in the target domain after optimization

[56] for fitting thermophysical models with RBF neural networks, the DNN with a structure of 42–512–218–64–4 and an initial learning rate of 0.0001 was trained for 20,000 iterations, and its MSE was 5.11e–4, which was less than the preset training target of 1e–3 and satisfied the convergence requirement. The regression analysis in Fig. 9 shows that the DNN-based surrogate model fit the traditional thermophysical model better than 90%, but there were many outliers, which resulted in very poor individual predictions; hence, the DNN-based surrogate model had to be optimized.

As described in Sect. 3.5, th Bayesian optimization algorithm was used to optimize the weights and bias of the DNN-based surrogate model for the spacecraft thermophysical model in this study and the optimized model was called the pre-training model for the next stage of transfer learning. In this study, an objective function, also called the score function, was set as follows for the Bayesian optimization algorithm to determine the optimal model:

$$\text{score} = \left(\frac{1}{\text{loss}_{\text{mean}}}\right) * 0.8 + \left(\frac{1}{\text{loss}_{\text{max}}}\right) * 0.2, \tag{10}$$

where $\text{loss}_{\text{mean}}$ denotes the mean error of the trained model and loss_{max} denotes the maximum error. With successive Bayesian optimizations, the scores increased exponentially, whereas the average and maximum errors of the model kept decreasing. After 264 iterations of training and optimization, the MSE of the obtained pre-training model reduced to 3.898e–5. Its regression analysis is shown in Fig. 10. Additionally, the computational speed of the pre-training model was 1000+ times faster than that of the traditional thermal physics model, and the computational accuracy was up to 99%+. Moreover, a very small number of outliers were identified; however, they were all within reasonable limits, as shown in Fig. 11.

Case 2: The cold case was considered as the source domain and the hot case as the target domain. Next, as in Case 1, the dataset of the source domain was obtained using PLHS and IBPS (see Fig. 12), a DNN-based surrogate model in

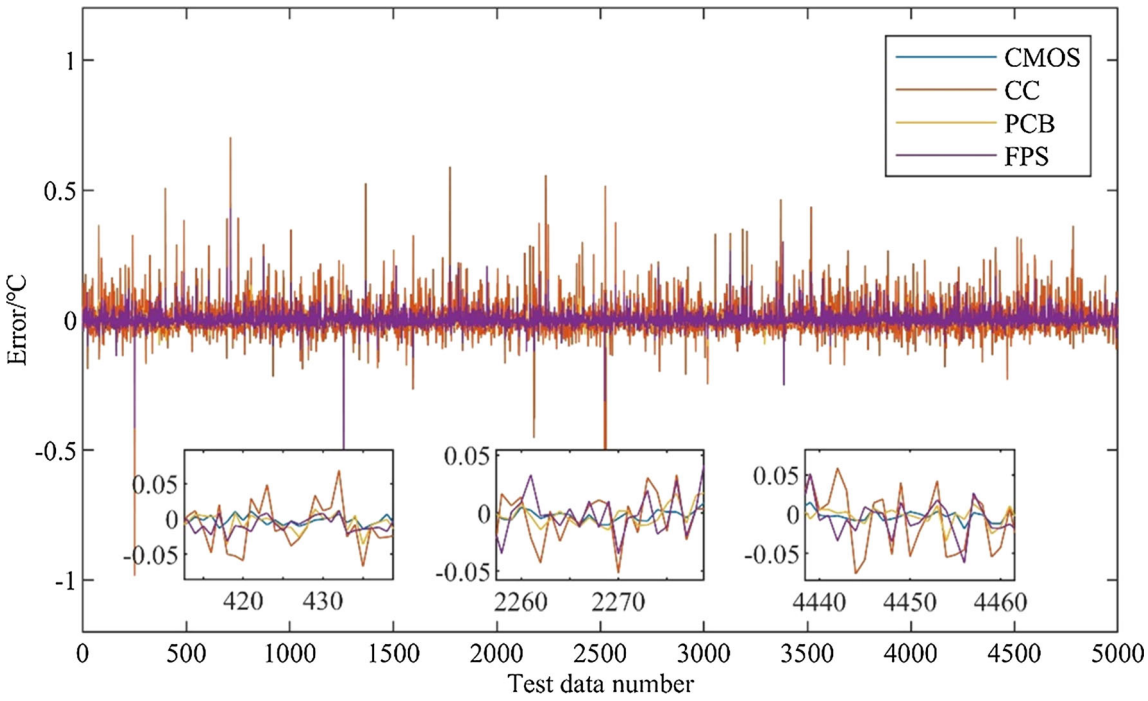

Fig. 15 Evaluation of the optimized pre-training model in the target domain

the source domain was built, and its hyperparameters were optimized using the Bayesian optimization algorithm from Ray.tune. The regression analysis of the DNN-based surrogate model before optimization is shown in Fig. 13. Clearly, the surrogate model also needed to be optimized. Similar to Case 1, the regression analysis of the DNN-based surrogate model in the source domain after Bayesian optimization is shown in Fig. 14. Clearly, the results after optimization were excellent, as shown in Fig. 15. Similar to Case 1, a very small number of outliers existed, but were within reasonable limits.

4.3.2 Transfer learning of the pre-training model in the target domain

Once the pre-training model in the source domain was obtained, the final, and crucial, step began: the pre-training model was further trained and optimized using transfer learning to adapt to the target domain.

Case 1: First, the surrogate model based on DNN for the spacecraft's thermophysical model was initialized in the target domain using the structure and hyperparameters of the pre-training model, and all the network parameters were not updated, except for the output layer, that is, the regression prediction layer weights. Then, the pre-trained model was trained using the limited training data in the target domain, where the limited training data in the target domain contained 5000 groups of samples in the range of values of the 42 thermal design parameters, as shown in Table 6, which were obtained using space thermal analysis with the support of PLHS and IBPS. The distribution of some parameters is shown in Fig. 16. The probability distribution laws of the parameters not shown in Fig. 16 were consistent with those of the parameters in Fig. 16. Next, convergence analysis was performed to evaluate the fitting performance of the DNN in the target domain after transfer learning, as shown in Fig. 17, and the accuracy reached 98%+; hence, there was no need for further optimization training. Finally, the pre-trained model after transfer learning was tested in the target domain, as shown in Fig. 18. The average error reached 0.03329K and the maximum error was 1.19047K, which was completely acceptable for the initial thermal design of the spacecraft.

Case 2: Similar to Case 1, the pre-training model in the source domain was selected as the initialized neural network structure for the surrogate model in the target domain, all hyperparameters, except the output layer, were fixed, and then, the pre-training model was trained using the limited training data in the target domain (5000 groups obtained in the same manner used in Case 1; the distribution of some parameters is shown in Fig. 19). After training was complete, convergence analysis was performed, as shown in Fig. 20, and the accuracy reached 98%+; hence, it was not necessary to train in optimization either. Finally, the pre-training model after transfer learning was tested in the target domain, as shown in Fig. 21. The average error reached 0.02089K and the maximum error reached

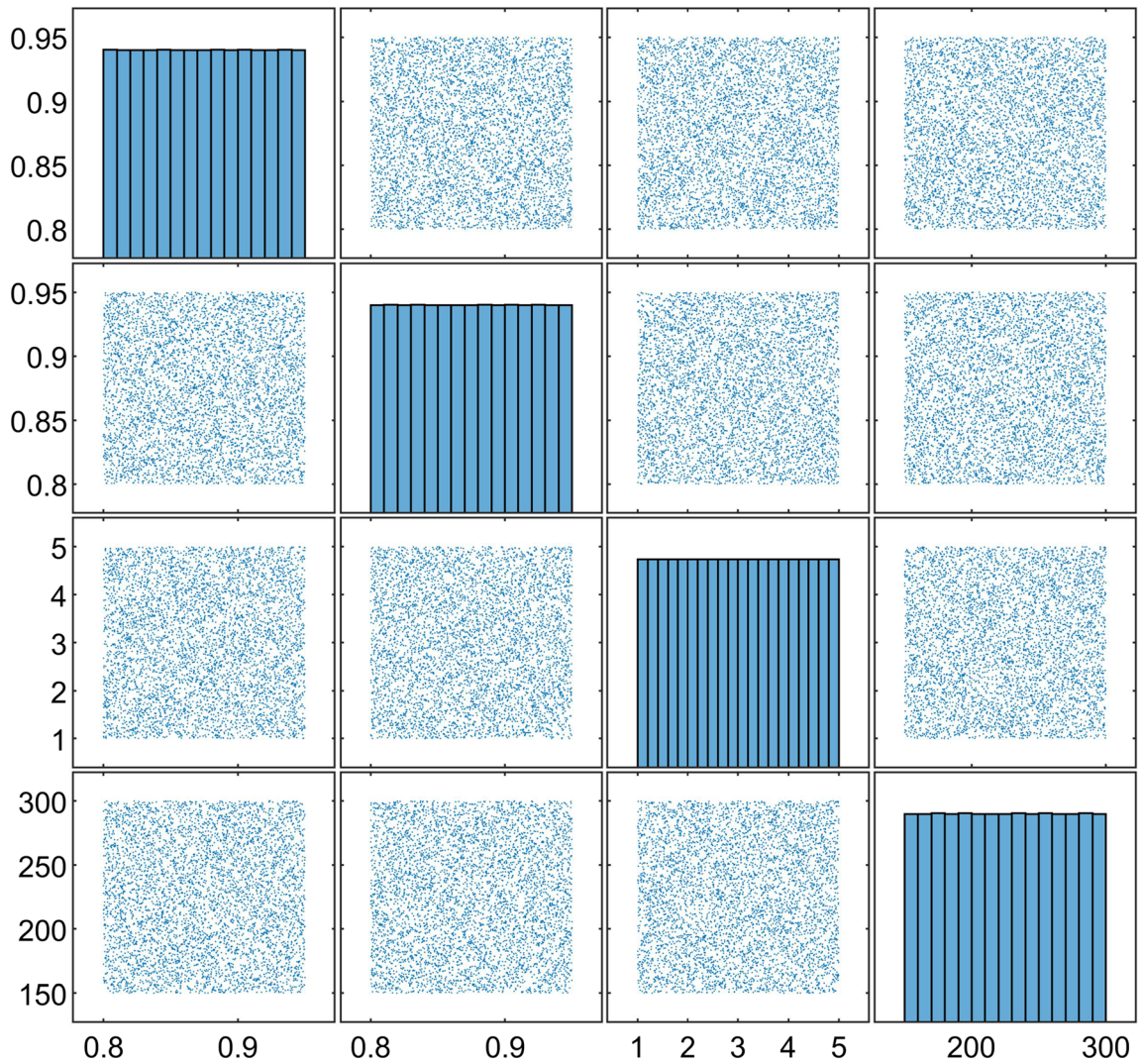

Fig. 16 Distribution of the DoE samples for transfer learning in Case 1

1.04138K, which was perfectly acceptable for the initial thermal design of the spacecraft.

5 Results

To improve the verification of the effect of transfer learning on surrogate modeling under multiple working conditions, the surrogate model in the target domain based on deep transfer learning (SMS-DL) was compared with the pre-trained model in the source domain (PMSD) and the surrogate model obtained from training in the target domain with limited training data (SMTD) for several metrics, such as prediction accuracy, maximum prediction error, and training dataset size.

Case 1: The comparative analysis of the prediction accuracy is shown in Fig. 22, and the other comparative analyses are shown in Table 8, where the mean error of different methods denotes the average value of the absolute error of the prediction output of the corresponding respective surrogate model, which we define as the prediction accuracy for the corresponding method in all following subsections. Clearly, the prediction accuracies of PMSD and SMTD were 0.24705K and 0.24523K, respectively, which were unacceptable, even in the initial thermal design stage of spacecraft with the lowest accuracy requirement, whereas the accuracy of SMS-DL reached 0.03329K, which was an improvement of 86.5% and 86.4% compared with those of PMSD and SMTD, respectively. The maximum prediction error of SMS-DL also reduced by 81.6% and 79.3% compared with those of PMSD and SMTD, respectively.

Case 2: The comparative analysis of the prediction accuracy is shown in Fig. 23, and the other comparative analyses are shown in Table 8. Clearly, the prediction accuracies of PMSD and SMTD were 0.24169K and

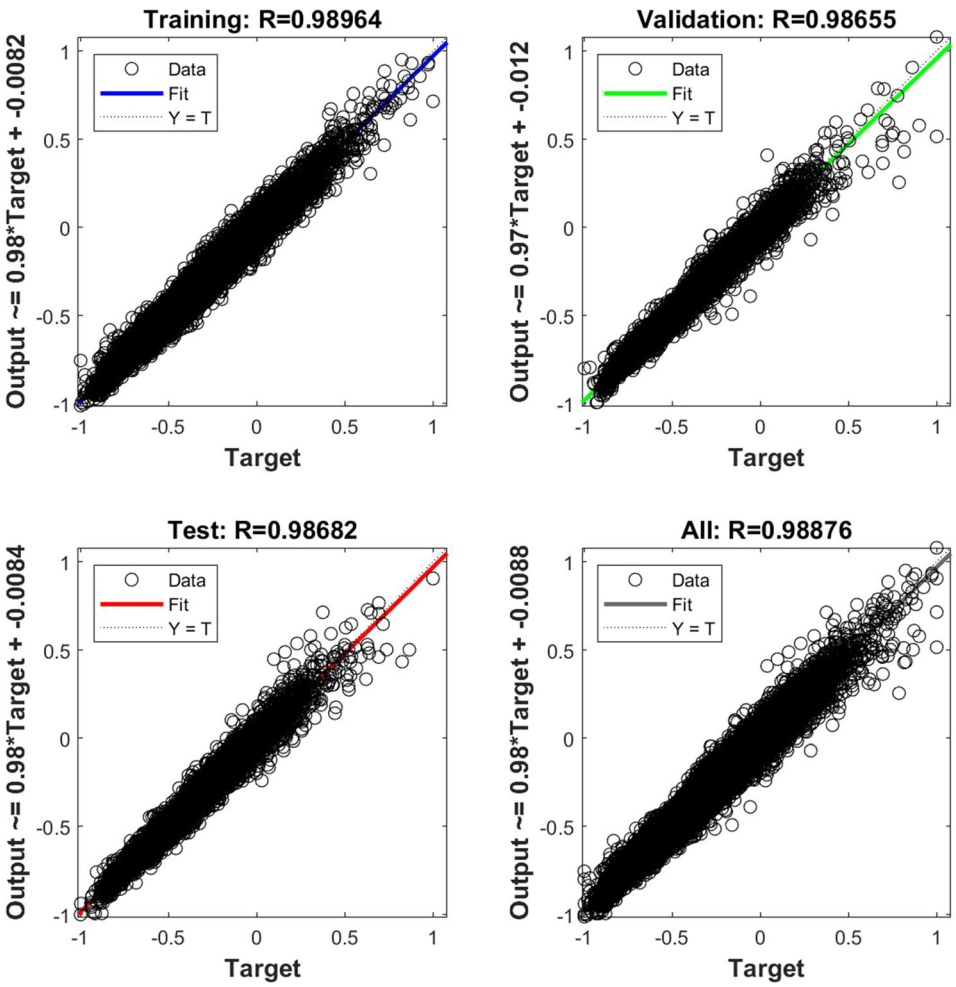

Fig. 17 Regression of the pre-training model in Case 1 after transfer learning

0.24149K, respectively, which were unacceptable, even in the initial thermal design stage of spacecraft with the lowest accuracy requirement, whereas the accuracy of SMS-DL reached 0.02089K, which was 91.4% and 91.3% higher than those of PMSD and SMTD, respectively. Simultaneously, the maximum error of SMS-DL also reduced by 84.0% and 84.1% relative to PMSD and SMTD, respectively.

6 Conclusions

An intelligent surrogate modeling strategy for spacecraft thermophysical models using deep learning was proposed in this study. This strategy used DNN as a surrogate model to reduce the computational cost of model evaluation. Additionally, using IBPS, which was specially designed for this study, an unsupervised real-time data interaction between text command data and analysis result data in various software such as MATLAB and NX TMG was achieved, which greatly improved the computational efficiency and avoided the risk of errors caused by manual operation.

During the specific application process, DNN was first combined with the Bayesian optimization algorithm to build a surrogate model for the thermophysical model of the spacecraft and then the surrogate model was trained in the target domain with limited tagging data after the feature space of the surrogate model in the source domain was preserved through transfer learning to adapt to the target domain. Then, regression analysis was performed to verify the fitting accuracy. If the accuracy was insufficient, the tagging data were increased appropriately or the optimization algorithm, such as the Bayesian optimization algorithm, was used to optimize the hyperparameters of the model to optimize the model.

Both the theoretical and experimental results demonstrated that deep transfer learning effectively adapted the pre-training model from one working condition to another, which improved the prediction accuracy by at least 86.4% over the direct prediction using the pre-training model from

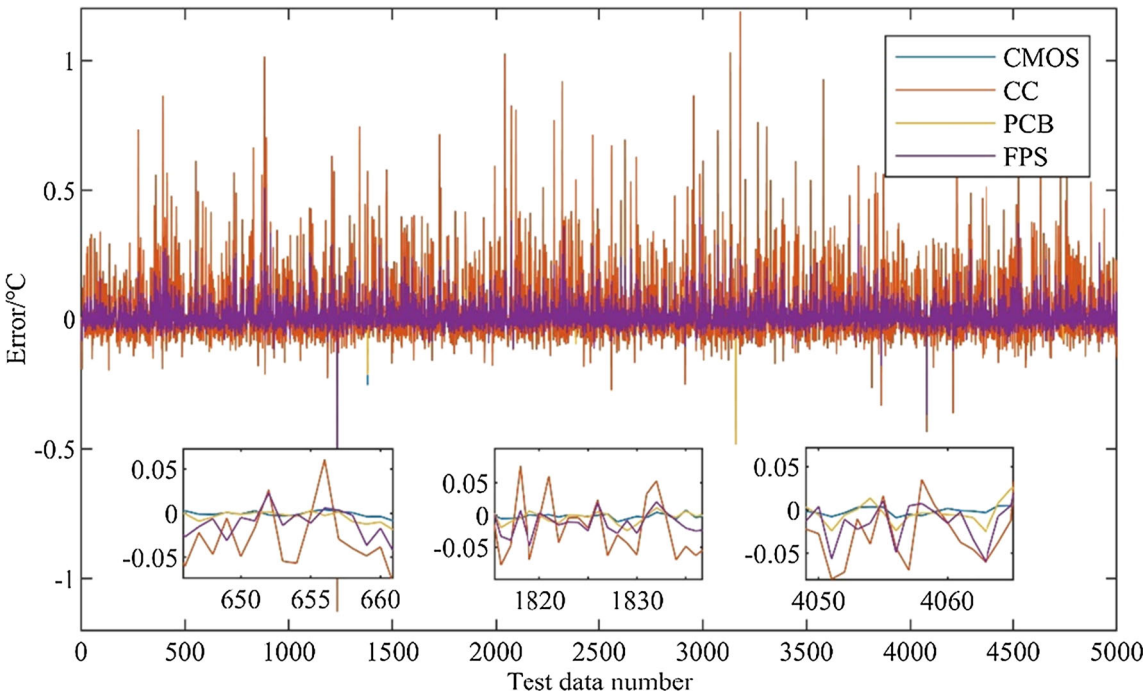

Fig. 18 Evaluation of the pre-training model in Case 1 after transfer learning

the source domain, and had better prediction performance than learning from scratch with limited data.

Furthermore, the proposed SMS-DL is not only applicable to surrogate modeling for thermophysical models of spacecraft but also a reference for other fields that also include finite element analysis-based modeling, such as force analysis.

The efficiency of the proposed SMS-DL was limited by the computational resources used (Intel Core i9-9900X CPU, 64 GB RAM, GeForce RTX 2080 Ti), which directly affected the time required for model computation. As computational resources are further improved, the computation time for surrogate modeling and model evaluation will be shortened, further easing the application of SMS-DL in space telescope thermal design optimization tasks. Additionally, the proposed SMS-DL is currently only applicable for model transfer across working conditions of homogeneous DNN, and further research is required on transfer learning for heterogeneous DNN across working conditions.

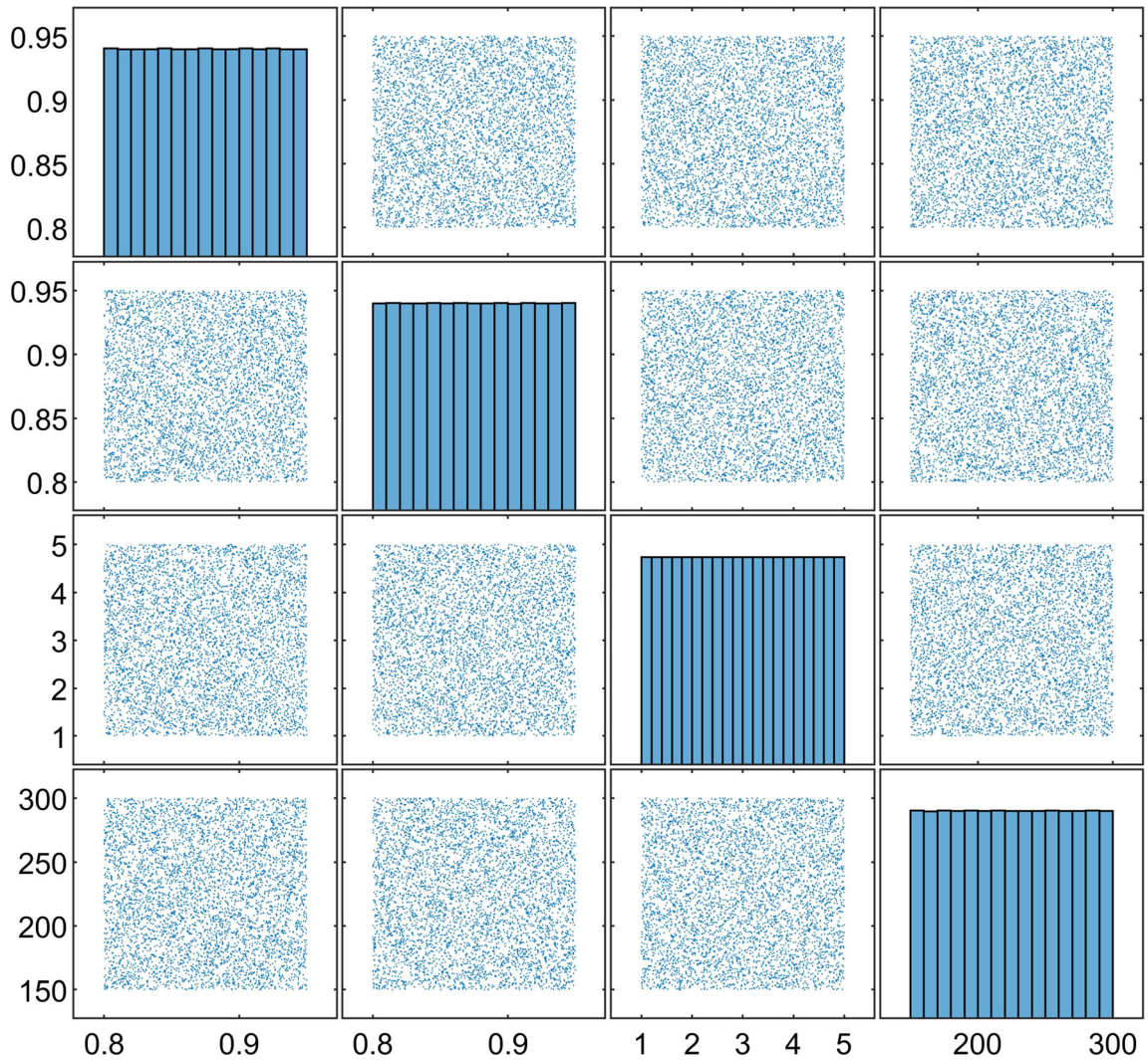

Fig. 19 Distribution of the DoE samples for transfer learning in Case 2

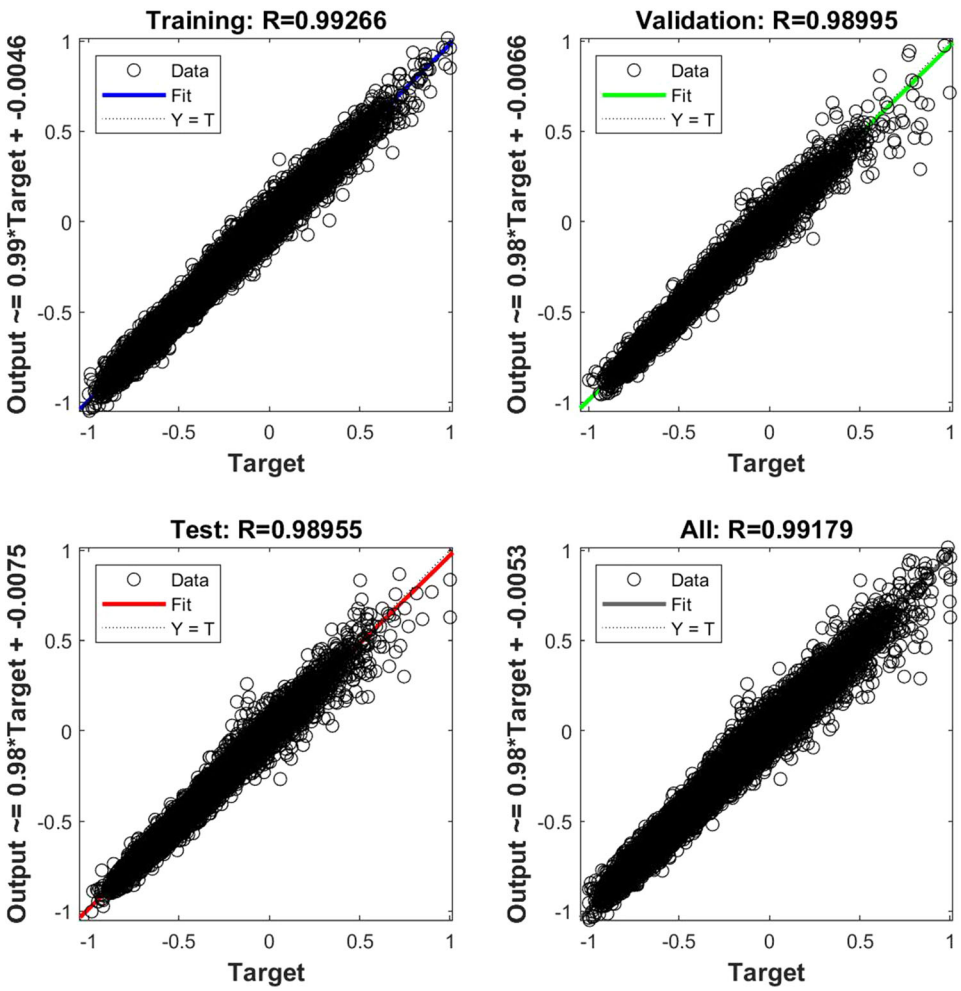

Fig. 20 Regression of the pre-training model in Case 2 after transfer learning

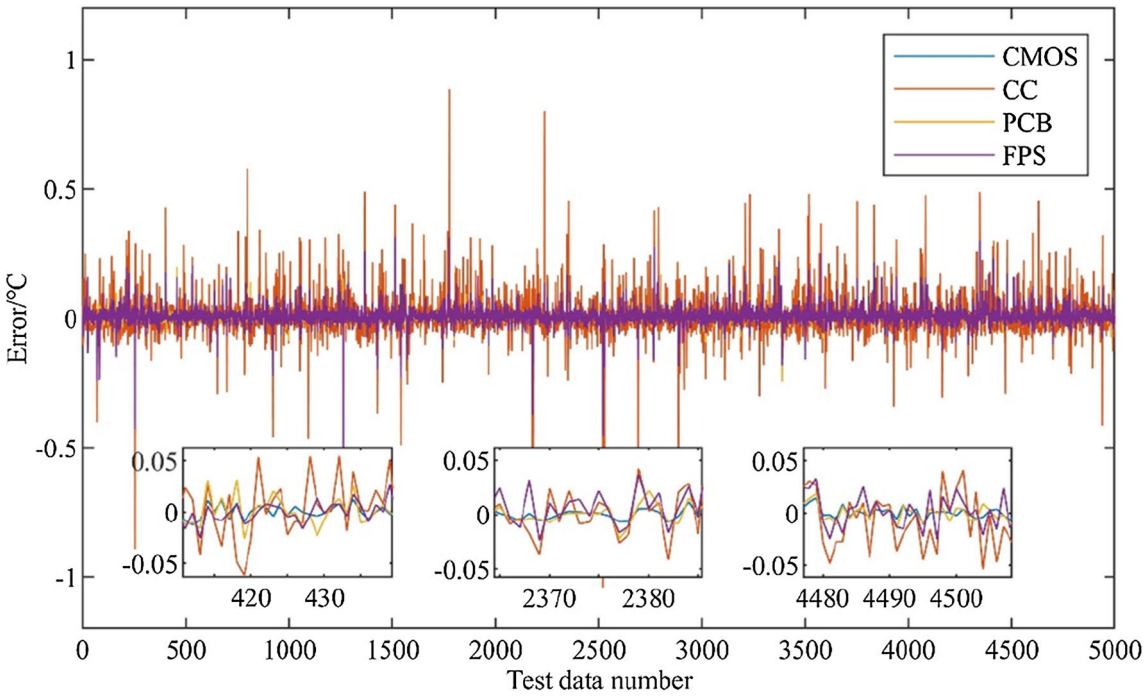

Fig. 21 Evaluation of the pre-training model in Case 2 after transfer learning

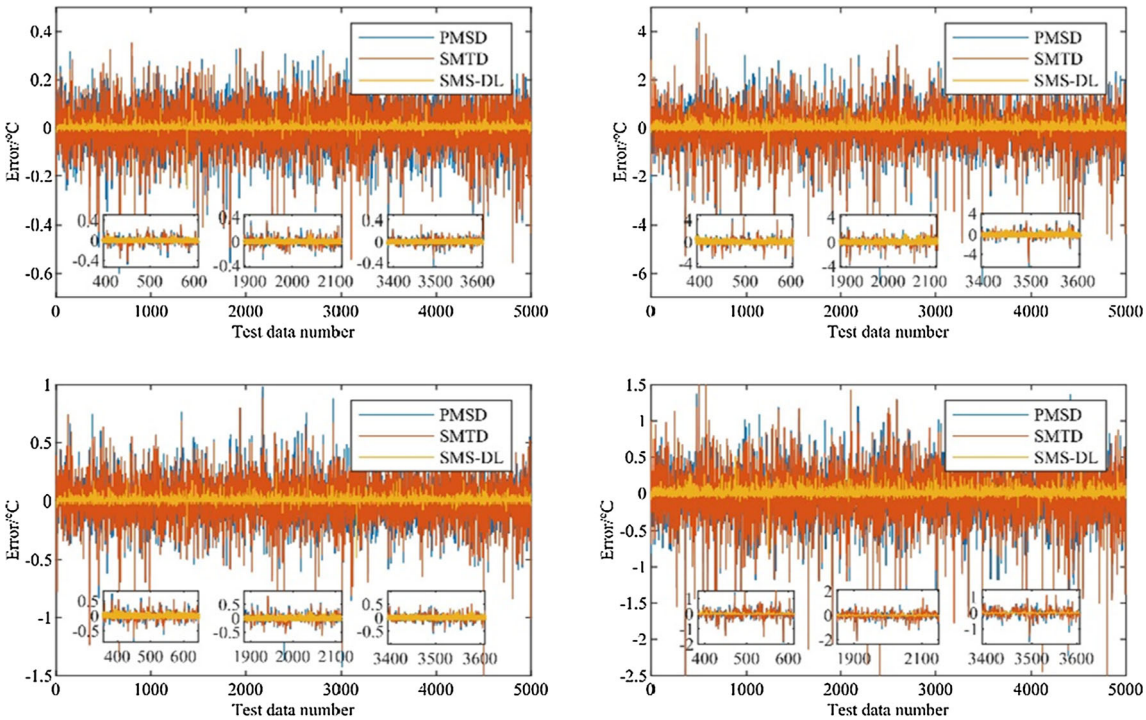

Fig. 22 Comparative analysis of different surrogate modeling methods in Case 1

Table 8 Comparison of the three methods

Parameter	SMS-DL		PMSD		SMTD	
	Case 1	Case 2	Case 1	Case 2	Case 1	Case 2
Neural network architecture	42–512–218–64–4		42–512–218–64–4		42–512–218–64–4	
Learning Rate	0.0001		0.0001		0.0005	
Loss function	HuberLoss		HuberLoss		MSELoss	
Optimization algorithms	Adam + Bayesian		Adam + Bayesian		SGD + Bayesian	
Mean error (CMOS/CC/PCB/FPS, °C)	0.00642	0.00642	0.06941	0.06639	0.06724	0.06652
	0.08057	0.04504	0.55469	0.54781	0.55529	0.54459
	0.01451	0.01141	0.12924	0.12423	0.12532	0.12812
	0.03165	0.02068	0.23486	0.22831	0.23307	0.22672
Max. absolute error (CMOS/CC/PCB/FPS, °C)	0.25439	0.14724	0.59958	0.96746	0.55354	0.86224
	1.19047	1.04138	6.46205	6.51857	5.76079	6.54647
	0.48361	0.24676	2.29191	1.52405	2.24433	1.51077
	0.81486	1.00112	3.26941	3.55497	2.90697	3.64094
Convergence speed (epochs)	1000	1000	0	0	20000	20000
Number of outliers (>1°C)	6	2	866	823	811	803
Total training time (s)	724.5	716.3	0	0	89245.5	8957.8

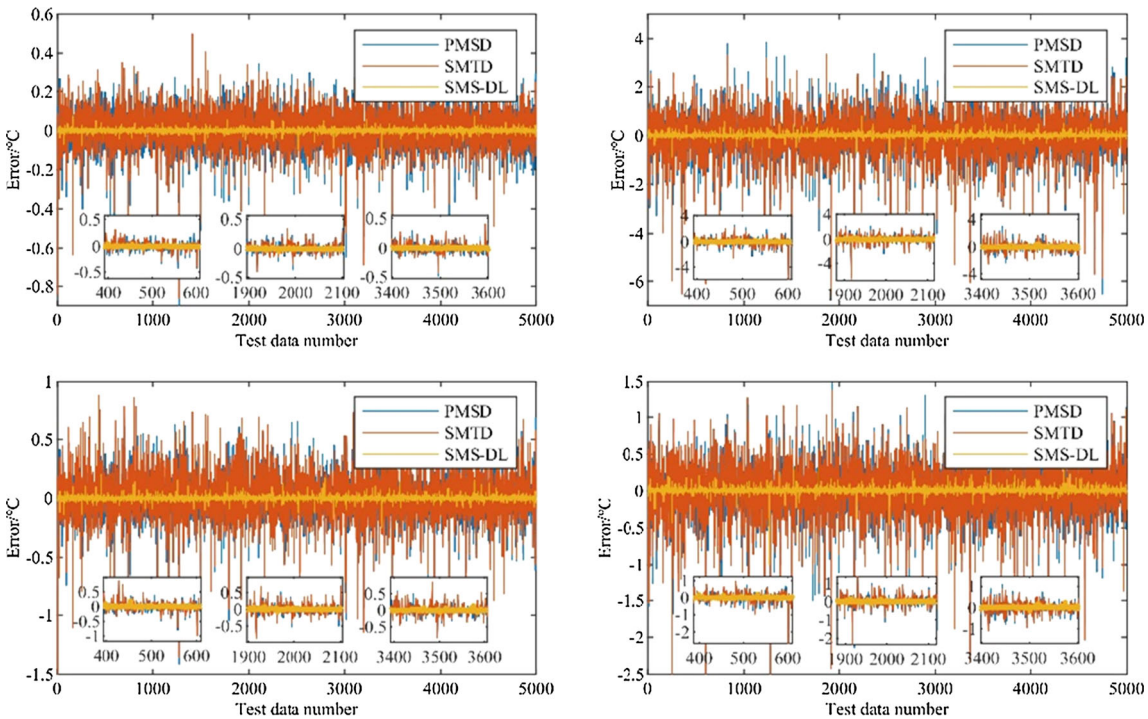

Fig. 23 Comparative analysis of different surrogate modeling methods in Case 2

Acknowledgements This work was supported by the National Natural Science Foundation of China (No. 61605203); and the Youth Innovation Promotion Association of the Chinese Academy of Sciences [No.2015173). We thank Maxine Garcia, PhD, from Edanz (https://jp.edanz.com/ac) for editing a draft of this manuscript.

Declarations

Conflict of interest The authors declare that they have no conflict of interest

References

1. Miao J, Zhong Q, Zhao Q, Zhao X (2021) Spacecraft thermal control technologies. Springer, Singapore
2. Meseguer J, Pérez-Grande I, Sanz-Andrés A (2012) Spacecraft thermal control. Elsevier, Cambridge
3. Chin J, Panczak T, Fried L (1992) Spacecraft thermal modelling. Int J Numer Meth Eng 35(4):641–653. https://doi.org/10.1002/nme.1620350403
4. Bulut M (2018) Thermal simulation software based on excel for spacecraft applications. Selçuk Üniversitesi Mühendislik, Bilim Ve Teknoloji Dergisi 6(4):592–600. https://doi.org/10.15317/Scitech.2018.154
5. Zhong Y-f, Zhu M-b, Wei F (2006) Application of i-deas in thermal-analysis of spacecraft. Comput Eng Design 12. https://doi.org/10.16208/j.issn1000-7024.2006.12.066
6. Panczak T, Rickman S, Fried L, Welch M (1991) Thermal synthesizer system: an integrated approach to spacecraft thermal analysis. SAE Trans 1851–1867
7. Liu L, Sun S, Cao D, Liu X (2019) Thermal-structural analysis for flexible spacecraft with single or double solar panels: A comparison study. Acta Astronaut 154:33–43. https://doi.org/10.1016/J.ACTAASTRO.2018.10.024
8. Lee S, Mudawar I, Hasan MM (2016) Thermal analysis of hybrid single-phase, two-phase and heat pump thermal control system (tcs) for future spacecraft. Appl Therm Eng 100:190–214. https://doi.org/10.1016/j.applthermaleng.2016.01.018
9. Shi R, Liu L, Long T, Liu J, Yuan B (2017) Surrogate assisted multidisciplinary design optimization for an all-electric geo satellite. Acta Astronaut 138:301–317. https://doi.org/10.1016/J.ACTAASTRO.2017.05.032
10. Wu Z, Huang Y, Chen X, Zhang X, Yao W (2018) Surrogate modeling for liquid-gas interface determination under microgravity. Acta Astronaut 152:71–77. https://doi.org/10.1016/J.ACTAASTRO.2018.07.001
11. Lal A, Raghunandan B (2005) Uncertainty analysis of propellant gauging system for spacecraft. J Spacecr Rocket 42(5):943–946. https://doi.org/10.2514/1.9511
12. Zheng Y, Yan C, Zhao Y (2020) Uncertainty and sensitivity analysis of inflow parameters for hyshot ii scramjet numerical simulaiton. Acta Astronaut 170:342–353. https://doi.org/10.1016/J.ACTAASTRO.2019.12.020
13. Saltelli A, Ratto M, Andres T, Campolongo F, Cariboni J, Gatelli D, Saisana M, Tarantola S (2008) Global sensitivity analysis: the primer. Wiley, London
14. Sun Y, Li F, Yang W, Yang J (2017) Thermal effects of optical antenna under the irradiation of laser. In: AOPC 2017: space optics and earth imaging and space navigation. International Society for Optics and Photonics, vol 10463, p 104631. https://doi.org/10.1117/12.2285378
15. Putz B, Wurster S, Edwards TEJ, Völker B, Milassin G, Többens DM, Semprimoschnig CO, Cordill MJ (2020) Mechanical and optical degradation of flexible optical solar reflectors during simulated low earth orbit thermal cycling. Acta Astronaut 175:277–289. https://doi.org/10.1016/J.ACTAASTRO.2020.05.032
16. Jiang Z, Lee YM (2019) Deep transfer learning for thermal dynamics modeling in smart buildings. In: 2019 IEEE international conference on Big Data (Big Data). IEEE, pp 2033–2037. https://doi.org/10.1109/BigData47090.2019.9006306
17. Asher MJ, Croke BF, Jakeman AJ, Peeters LJ (2015) A review of surrogate models and their application to groundwater modeling. Water Resour Res 51(8):5957–5973. https://doi.org/10.1002/2015WR016967
18. Buhmann MD (2000) Radial basis functions. Acta Numerica 9:1–38. https://doi.org/10.1017/S0962492900000015
19. Blanning RW (1975) The construction and implementation of metamodels. Simulation 24(6):177–184. https://doi.org/10.1177/003754977502400606
20. Willcox K, Peraire J (2002) Balanced model reduction via the proper orthogonal decomposition. AIAA J 40(11):2323–2330. https://doi.org/10.2514/2.1570
21. O'Hagan A (2006) Bayesian analysis of computer code outputs: a tutorial. Reliab Eng Syst Saf 91(10–11):1290–1300. https://doi.org/10.1016/j.ress.2005.11.025
22. Stein ML (1999) Interpolation of spatial data: some theory for kriging. Springer, New York
23. Bieker HP, Slupphaug O, Johansen TA (2007) Real-time production optimization of oil and gas production systems: a technology survey. SPE Prod Oper 22(04):382–391. https://doi.org/10.2118/99446-PA
24. Yang D-C, Jang I-S, Jang M-H, Park C-N, Park C-J, Choi J (2009) Optimization of additive compositions for anode in ni-mh secondary battery using the response surface method. Met Mater Int 15(3):421–425. https://doi.org/10.1007/s12540-009-0421-0
25. Mohammadi-Amin M, Entezari MM, Alikhani A (2018) An efficient surrogate-based framework for aerodynamic database development of manned reentry vehicles. Adv Space Res 62(5):997–1014
26. Peter T (2018) Using deep learning as a surrogate model in multi-objective evolutionary algorithms. Otto-von-Guericke-Universität, Magdeburg
27. Chen X, Zhao X, Gong Z, Zhang J, Zhou W, Chen X, Yao W (2021) A deep neural network surrogate modeling benchmark for temperature field prediction of heat source layout. Preprint at https://arxiv.org/abs/2103.11177
28. Hutzenthaler M, Jentzen A, Kruse T, Anh Nguyen T, von Wurstemberger P (2020) Overcoming the curse of dimensionality in the numerical approximation of semilinear parabolic partial differential equations. Proc R Soc A 476(2244):20190630. https://doi.org/10.1098/rspa.2019.0630
29. Hutzenthaler M, Jentzen A, Kruse T, Nguyen TA (2020) A proof that rectified deep neural networks overcome the curse of dimensionality in the numerical approximation of semilinear heat equations. SN Partial Differ Equ Appl 1(2):1–34. https://doi.org/10.1007/s42985-019-0006-9
30. Grohs P, Hornung F, Jentzen A, Von Wurstemberger P (2018) A proof that artificial neural networks overcome the curse of dimensionality in the numerical approximation of Black-Scholes partial differential equations. Preprint at https://arxiv.org/abs/2103.11177
31. Vasudevan RK, Ziatdinov M, Vlcek L, Kalinin SV (2021) Off-the-shelf deep learning is not enough, and requires parsimony, bayesianity, and causality. NPJ Comput Mater 7(1):1–6. https://doi.org/10.1038/s41524-020-00487-0
32. Peng H, Wang W (2016) Adaptive surrogate model based multi-objective transfer trajectory optimization between different

libration points. Adv Space Res 58(7):1331–1347. https://doi.org/10.1016/j.asr.2016.06.023
33. Xiong Y, Guo L, Huang Y, Chen L (2020) Intelligent thermal control strategy based on reinforcement learning for space telescope. J Thermophys Heat Transfer 34(1):37–44. https://doi.org/10.2514/1.t5774
34. Huang H, Xie X, Gu J (2020) Modelling and analysis of spacecraft external heat flux environment for the solar array. Spacecraft Environ Eng 37(3):275–279. https://doi.org/10.12126/see.2020.03.011
35. Li J, Yan S, Cai R (2013) Thermal analysis of composite solar array subjected to space heat flux. Aerosp Sci Technol 27(1):84–94. https://doi.org/10.1016/j.ast.2012.06.010
36. Huabin Y, Qingwen W, Liheng C, Fei H, Xusheng Z (2015) Calculation of external heat fluxes on space camera with changing attitudes frequently in geomagnetic coordinate system. Infrared Laser Eng 44(6):1923–1928
37. Pan SJ, Zheng VW, Yang Q, Hu DH (2008) Transfer learning for wifi-based indoor localization. In: Association for the Advancement of Artificial Intelligence (AAAI) workshop, vol 6. The Association for the Advancement of Artificial Intelligence Palo Alto
38. Motiian S, Piccirilli M, Adjeroh DA, Doretto G (2017) Unified deep supervised domain adaptation and generalization. In: Proceedings of the IEEE international conference on computer vision, pp 5715–5725
39. Conneau A, Kiela D, Schwenk H, Barrault L, Bordes A (2017) Supervised learning of universal sentence representations from natural language inference data. Preprint at https://arxiv.org/abs/1705.02364
40. Muandet K, Balduzzi D, Schölkopf B (2013) Domain generalization via invariant feature representation. In: International conference on machine learning. PMLR, pp 10–18
41. Xiong Y, Guo L, Tian D, Zhang Y, Liu C (2020) Intelligent optimization strategy based on statistical machine learning for spacecraft thermal design. IEEE Access 8:204268–204282. https://doi.org/10.1109/ACCESS.2020.3036548
42. Peeters J, Van Houtte J, Martinez A, van Muiden J, Dirckx J, Steenackers G (2016) Determination of stratospheric component behaviour using finite element model updating. Aerosp Sci Technol 56:22–28. https://doi.org/10.1016/j.ast.2016.06.024
43. Knutson KJ, Briggs C (2005) Innovative computing techniques for nx analysis and post processing to fill emerging needs
44. Azarkish H, Rashki M (2019) Reliability and reliability-based sensitivity analysis of shell and tube heat exchangers using monte carlo simulation. Appl Therm Eng 159:113842. https://doi.org/10.1016/j.applthermaleng.2019.113842
45. Chen X, Chen X, Zhou W, Zhang J, Yao W (2020) The heat source layout optimization using deep learning surrogate modeling. Struct Multidiscip Optim 62(6):3127–3148. https://doi.org/10.1007/s00158-020-02659-4
46. Sun L, Gao H, Pan S, Wang J-X (2020) Surrogate modeling for fluid flows based on physics-constrained deep learning without simulation data. Comput Methods Appl Mech Eng 361:112732. https://doi.org/10.1016/j.cma.2019.112732
47. Marcelino P (2018) Transfer learning from pre-trained models. Towards Data Science
48. Jasper Snoek RPA, Hugo Larochelle (2012) Practical bayesian optimization of machine learning algorithms. Preprint at https://arxiv.org/abs/1206.2944
49. Inkawich N (2021) Finetuning Torchvision Models - PyTorch Tutorials 1.2.0 documentation. https://pytorch.org/tutorials/beginner/finetuning_torchvision_models_tutorial.html. Accessed 29 Aug 2021
50. Pan SJ, Tsang IW, Kwok JT, Yang Q (2010) Domain adaptation via transfer component analysis. IEEE Trans Neural Networks 22(2):199–210. https://doi.org/10.1109/TNN.2010.2091281
51. Li W, Xiao M, Peng X, Garg A, Gao L (2019) A surrogate thermal modeling and parametric optimization of battery pack with air cooling for evs. Appl Therm Eng 147:90–100
52. Fang K-T, Lin DK, Winker P, Zhang Y (2000) Uniform design: theory and application. Technometrics 42(3):237–248. https://doi.org/10.1080/00401706.2000.10486045
53. Box GE (1954) The exploration and exploitation of response surfaces: some general considerations and examples. Biometrics 10(1):16–60. https://doi.org/10.2307/3001663
54. McKay MD, Beckman RJ, Conover WJ (2000) A comparison of three methods for selecting values of input variables in the analysis of output from a computer code. Technometrics 42(1):55–61. https://doi.org/10.1080/00401706.2000.10485979
55. Zhou W-H, Yuen K-V, Tan F (2013) Estimation of maximum pullout shear stress of grouted soil nails using bayesian probabilistic approach. Int J Geomech 13(5):659–664. https://doi.org/10.1061/(ASCE)GM.1943-5622.0000259
56. Xiong Y, Guo L, Yang Y, Wang H (2021) Intelligent sensitivity analysis framework based on machine learning for spacecraft thermal design. Aerosp Sci Technol 118:106927. https://doi.org/10.1016/j.ast.2021.106927
57. Sheikholeslami R, Razavi S (2017) Progressive Latin hypercube sampling: an efficient approach for robust sampling-based analysis of environmental models. Environ Model Softw 93:109–126. https://doi.org/10.1016/j.envsoft.2017.03.010
58. Tan C, Sun F, Kong T, Zhang W, Yang C, Liu C (2018) A survey on deep transfer learning. In: International conference on artificial neural networks. Springer, pp 270–279
59. Barnett SM, Ceci SJ (2002) When and where do we apply what we learn? A taxonomy for far transfer. Psychol Bull 128(4):612. https://doi.org/10.1037/0033-2909.128.4.612
60. Pan SJ, Yang Q (2009) A survey on transfer learning. IEEE Trans Knowl Data Eng 22(10):1345–1359. https://doi.org/10.1109/TKDE.2009.191
61. Inc., TM (2021) MATLAB - MathWorks - MATLAB & Simulink. https://ch.mathworks.com/de/products/matlab.html?s_tid=hp_products_matlab. Accessed 6 Sept 2021
62. Mallapaty S (2021) China's space station is preparing to host 1000 scientific experiments. Nature 22(596):20–21. https://doi.org/10.1038/d41586-021-02018-3
63. Zhan H (2019) An update on the Chinese space station telescope project. In: ISSI-BJ Workshop: Weak Gravitational Lensing Studies from Space Missions, Beijing, pp 270–279
64. Zhan H (2018) An overview of the Chinese space station optical survey. In: 42nd COSPAR Scientific Assembly, Beijing, pp 1–16
65. Xiong Y, Guo L, Tian D (2021) Application of deep reinforcement learning to thermal control of space telescope. J Therm Sci Eng Appl. https://doi.org/10.1115/1.4051072
66. Mahan JR (2019) The Monte Carlo Ray-trace method in radiation heat transfer and applied optics. Wiley, West Sussex
67. Michael D, Suderlandb M, Reissb P, Czupallac M (2015) Development and evaluation of thermal model reduction algorithms for spacecraft. Acta Astronaut 110:168–179. https://doi.org/10.1016/j.actaastro.2015.01.018
68. Liaw R, Liang E, Nishihara R, Moritz P, Gonzalez JE, Stoica I (2018) Tune: a research platform for distributed model selection and training. Preprint at https://arxiv.org/abs/1807.05118
69. PyTorch: Welcome to PyTorch Tutorials - PyTorch Tutorials 0.3.1.post2 documentation (2021). https://pytorch.org/tutorials/. Accessed 10 Sept 2021